Aus dem Institut für Normale und Pathologische Physiologie
Geschäftsführender Direktor: Prof. Dr. Dr. J. Daut,
Abteilung für Zellphysiologie: Leiter Prof. Dr. Dr. J. Daut

des Fachbereichs Medizin der Philipps-Universität Marburg und des
Universitätsklinikums Giessen und Marburg, Standort Marburg

The stretch-activated potassium channel TREK-1 in rat cardiac ventricular muscle

Inaugural-Dissertation zur Erlangung des Doktorgrades

Dr. rer. physiol.

Dem Fachbereich Medizin der Philipps-Universität Marburg vorgelegt von

Xiantao Li aus Hubei (China).

Marburg, 2005

Angenommen vom Fachbereich Humanmedizin der Philipps-Universität Marburg am 25.11.2005, gedruckt mit Genehmigung des Fachbereichs.
Dekan: Prof. Dr. B. Maisch
Referent: Prof. Dr. Dr. J. Daut
Correferent: Prof. Dr. T. Gudermann

Contents

Introduction

1. Tandem pore domain potassium channels

Potassium channels are protein complexes that form K^+ selective pores in biological membranes and are the largest family of ion channels among all ion channels in the human genome. There exists a common motif G(Y/F/L)G in all potassium channels, which is essential for forming a functional potassium conducting pore.

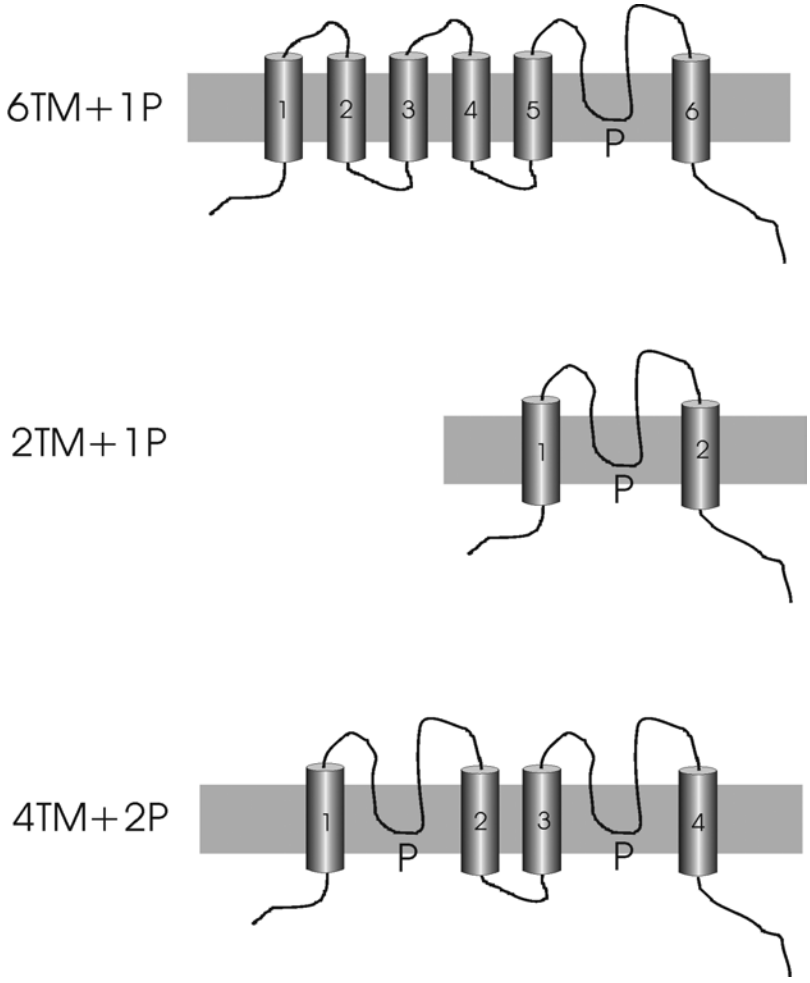

Figure 1. Molecular structure of K^+ channel subunits
Molecular structure of K^+ channel subunits. Top, subunit with six transmembrane segments (M1–M6) and one pore domain encodes voltage gated K^+ channels. P represents the pore-loop. Middle, subunits with two transmembrane segments (M1, M2) and one pore loop encode inward rectifying K^+ channels. Bottom, subunits with four transmembrane segments (M1-M4) and two pore domains (P1, P2) encode K_2P channels.

Mammalian potassium channel are classified into three groups according to their membrane topology (Fig. 1): 6 transmembrane segments (TM)/1 pore domain (P), 2TM/1P and 4TM/2P (tandem domain K^+ channel, K_2P). 6TM/1P encode voltage-gated potassium channels. 2TMS/1P encode inward rectifying potassium channels. 4TM/2P encode the background potassium channels. Background channels was also called leak channels because it was originally thought those channels have not time and voltage dependence and can open at resting membrane potential. The currents carried out by K_2P channels are probably larger at depolarized potentials. Background K_2P channels play an important role in control of potassium homeostasis, cell volume, setting the membrane potential and tuning the action potential.

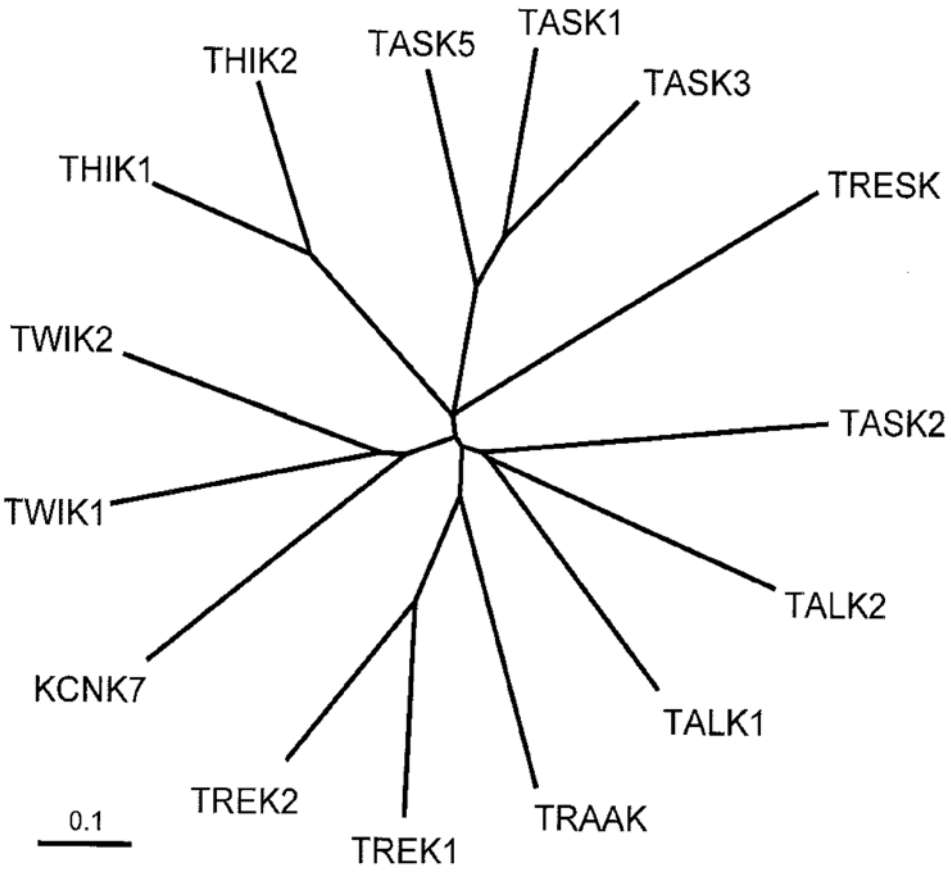

Figure 2. Phylogenetic tree of the human two-pore domain potassium channel family

The tree was generated using the neighbor-joining algorithm of the Phylip program on the basis of a multiple alignment of conserved sequences of the pore-forming domain analyzed with the ClustalW program (Sano et al., 2003).

The class of mammalian 4TM/2P background potassium channels consist so far of 15 members and are classified into several subfamilies (Fig. 2): (1) TWIK-1, TWIK-2 and KCNK7; (2) acid-sensitive TASK-1 and TASK-3; (3) mechano-sensitive TREK-1, TREK-2 and TRAAK; (4) alkaline-activated TASK-2, TALK-1 and TALK-2; (5) THIK-1 and THIK-2; (6) TRESK. So following presentation is brief property of two pore domain potassium channels.

1.1 Weakly inward rectifier TWIK-1 and TWIK-2

TWIK channels are widely expressed in many tissue types (Arrighi et al., 1998). TWIK-1 is highly expressed in the brain (Lesage et al., 1997). When expressed in heterologous expression systems, both TWIK-1 and TWIK-2 produce potassium currents of weak amplitude (Chavez et al., 1999; Lesage et al., 1996; Lesage et al., 1997). TWIK-1 has a unitary conductance of 34 pS with flickery behavior in symmetrical 140 mM KCl (Lesage et al., 1996). TWIK-1 but not TWIK-2 is blocked by Ba^{2+}, quinine, and quinidine. Both channels are only slightly or not at all sensitive to the classic potassium channel blockers tetraethylammonium (TEA), 4-aminopyridine (4-AP), and Cs^{+}. PKC activation increases the TWIK currents, whereas acidification inhibits them. TWIK-1 and TWIK-2 are not sensitive to changes in extracellular pH and to treatments that activate protein kinase A (PKA).

But other groups did not observe the activity of TWIK-1 (Orias et al., 1997; Goldstein et al., 1998). The recent study suggested TWIK-1 was inactive despite residence in the plasma membrane so long as the protein is covalently modified by small ubiquitin-ralated modifier protein (SUMO). SUMO-conjugation enzyme assembled with TWIK-1 and kept it silent. Removal of SUMO by SUMO protease can activate TWIK-1 channels (Rajan et al., 2005). The function of TWIK-1 channels were unknown and some results from TWIK-1 knock-out mice indicated it may contribute to the regulation of renal phosphate (Pi) transport in proximal tubule and water transport in medullary collecting duct (Nie et al., 2005).

1.2 Acid-sensitive TASK-1 and TASK-3

TASK-1 is strongly expressed in the brain, for example in cerebellar granule neurons, somatic motoneurons and the locus coeruleus. TASK-3 is more widely distributed in the brain and is highly expressed in somatic motoneurons, cerebellar granule neurons, the locus coeruleus and raphe nuclei, and in various nuclei of the thalamus and hypothalamus (Talley et al., 2001; De Miera et al., 2001; Karschin et al., 2001). In the peripheral tissues, TASK channel mRNA has also been found in heart (Duprat et al., 1997; Kim et al., 1998; Lopes et al., 2000; Kim et al., 1999), a neuroepithelial body cell line (Hartness et al., 2001; O'Kelly et al., 1999), carotid body glomus cells (Buckler et al., 2000), adrenal gland (Czirjak et al., 2000; 2002), and kidney (Kim et al., 2000).

TASK-1 and TASK-3 can generate pH-sensitive whole-cell K^+ currents with little time-dependence and outward rectification. In symmetric K^+ solutions, the unitary conductance of TASK-1 channels (~14 pS) is about one-half that of TASK-3 channels (~28 pS), although kinetics and voltage-dependence of these two TASK channels are very similar (Duprat et al., 1997; Kim et al., 1998; Kim et al., 2000; Rajan et al., 2000; Lopes et al., 2000). Cell-attached patch-clamp recordings of TASK-3 expressed in HEK293 cells showed that the single channel current-voltage relation was inwardly rectifying, and open probability increased markedly with depolarization. The outward rectification found in the whole-cell currents may be reconciled with the inward rectification of the single K^+ channels by taking into account the marked increase in open probability observed at positive potentials (Rajan et al., 2000).

TASK-1 and TASK-3 can be distinguished from one another by the pH range over which their activity is modulated. Thus, the pK for inhibition of TASK-1 channels is ~7.4, in the physiological range, whereas the TASK-3 channel is inhibited at a more acidic pH, with a pK ~6.7 (Duprat et al., 1997; Kim et al., 1998; Kim et al., 2000; Rajan et al., 2000; Lopes et al., 2000). In addition to differences in pH sensitivity, TASK-1 and TASK-3 channels are also reported to be differentially sensitive to block by ruthenium red, zinc, or anandamide. Ruthenium red blocks TASK-3 at concentrations that do not inhibit TASK-1 (Czirjak et al., 2002; 2003). Zinc selectively block TASK-3 but not TASK-1 (Clarke et al., 2004)

Human TASK-1 was also reported to be blocked by the endocannabinoid anandamide (Maingret et al., 2001). Local anesthetics such as lidocaine and bupivacaine inhibited TASK channels (Leonoudakis et al., 1998; Meadows et al., 2001). The cloned human TASK-1 channel is modestly inhibited by hypoxia (Lewis et al., 2001).

1.3 Mechano-sensitive TREK-1, TREK-2 and TRAAK

At present, there are three members of the mechano-sensitive TREK subfamily: TREK-1, TREK-2 and TRAAK. The basic characteristics of TREK-like potassium channels are their sensitivity to unsaturated free fatty acids, pressure and intracellular acidosis (Kim, 2003; Patel et al., 2001). Other properties are flicking behavior with low sensitivity to K^+ channel blockers such as tetraethylammonium (TEA) or barium.

There are different expression levels of three mechano-sensitive K^+ channels in human. All three mechano-sensitive K^+ channels are found to be expressed in many parts of the brain (Medhurst et al., 2001). Outside of CNS, TREK-1 mRNA is strongly expressed in the ovary, stomach, small intestine and myometrium (Bai et al., 2005) but at very low levels in other tissues. TREK-2 mRNA is highly found in the brain and kidney and low levels at other tissue. TRAAK mRNA is detected in placenta. In other species such as rat and mouse, three mechano-sensitive K^+ channels were detected in brain. In the peripheral tissue, TREK-1 also was found in heart.

TREK-1 and TREK-2, but not TRAAK, are activated by clinically relevant concentrations of inhalation anesthetics such as halothane and isoflurane (Patel et al., 1999). Like TREK-1 and TREK-2, TRAAK is activated by free fatty acids and membrane stretch. However, TRAAK is activated by alkaline rather than acid conditions (Kim et al., 2001). The local anesthetic agent bupivacaine inhibits TREK and TASK (Kim et al., 2000; Punka et al., 2003). Both TREK-1 and TREK-2 are activated by heat and inhibited by cold. Riluzole, a neuroprotective agent, is reported to activate TREK-1 and TRAAK (Duprat et al., 2000). However, sipatrigine, another neuroprotective agent, significantly inhibits these channels (Meadows et al., 2001).

1.4 Alkaline-activated TASK-2, TALK-1 and TALK-2

TALK-1a is a member of the K_2P channel family and was first isolated from human pancreas cDNA (Girard et al., 2001). The first two subunits, TALK-1 and TALK-2, are related to TASK-2. The corresponding channels produce non-inactivating currents that are activated at alkaline pH. These currents are sensitive to Ba^{2+}, quinine, quinidine, chloroform, halothane, and isoflurane but are not affected by TEA, 4-AP, Cs^+, arachidonic acid, hypertonic solutions, agents activating protein kinases C and A, changes of internal Ca^{2+} concentrations, and by activation of Gi and Gq proteins. TALK-1 is exclusively expressed in the pancreas. TALK-2 is mainly expressed in the pancreas, but is also expressed at a lower level in liver, placenta, heart, and lung (Girard et al., 2001).

The conductance of TASK-2 was estimated to be 14.5 pS in physiological conditions and 59.9 pS in symmetrical conditions with 155 mM K^+. Quinine and quinidine blocked TASK-2 currents but the other classical K^+ channel blockers tetraethylammonium, 4-aminopyridine, and Cs^+ do not affect TASK-2. TASK-2 channels are only slightly sensitive to Ba^{2+}. Like TASK-1, TASK-2 is highly sensitive to external pH in the physiological range. Unlike all other cloned K_2P channels, TASK-2 is essentially absent in the brain. In human and mouse, TASK-2 is mainly expressed in the kidney, where in situ hybridization shows that it is localized in cortical distal tubules and collecting ducts. TASK-2 expression levels in uterus, lung and pancreas are different between human and mouse. The localization and functional properties of TASK-2 indicates that it may play an essential role in renal K^+ transport (Reyes et al., 1998).

1.5 Halothane-inhibited THIK-1 and THIK-2

Heterologous expression of rTHIK-1 in Xenopus oocytes revealed a K^+ channel displaying weak inward rectification in symmetrical K^+ solution. The current was enhanced by arachidonic acid and inhibited by halothane. rTHIK-2 did not functionally express (Rajan et al., 2000). Hypoxia reversibly inhibited THIK-1 currents and caused membrane depolarization. THIK-1 may play a physiological and/or pathological role during brain ischemia (Campanucci et al., 2005).

1.6 TRESK

RT-PCR results suggest that TRESK is expressed in the spinal cord. TRESK shows outward rectification and functions as a background K^+ channel. TRESK was inhibited by previously reported K^+ channel inhibitors Ba^{2+}, propafenone, glibenclamide, lidocaine, quinine, quinidine, and triethanolamine. TRESK was also inhibited by unsaturated free fatty acids such as arachidonic acid and docosahexaenoic acid. TRESK is sensitive to changes in extracellular and intracellular pH. These properties indicate that TRESK is a novel two-pore domain K^+ channel that may set the resting membrane potential of cells in the spinal cord (Sano et al., 2003).

A new K_2P channel named TRESK-2 has been isolated from mouse testis complementary DNA, which its amino acid sequence shares 65% identity with that of TRESK-1. Northern blot analysis suggested rat TRESK-2 mRNA was expressed strongly in the thymus and spleen and at low levels in many other tissues, including heart, small intestine, skeletal muscle, uterus, testis, and placenta. TRESK-2 mRNA is also expressed in mouse and human tissues. A time-independent and non-inactivating K^+-selective current was recorded in COS-7 cells transfected with TRESK-2 DNA. TRESK-2 was insensitive to 1 mM tetraethylammonium, 100 nM apamin, 1 mM 4-aminopyridine, and 10 μM glibenclamide. TRESK-2 was also blocked by 10 μM quinidine, 20 μM arachidonate and acid (pH 6.3). The current-voltage relationship of TRESK-2 was weakly inwardly rectifying in symmetrical 150 mM KCl. The single channel conductance is 13 pS at +60 mV and 16 pS at -60 mV (Kang et al., 2004).

2. Cardiac K_2P channels

Cardiac potassium channels carry outward currents and act either to set the resting potential near the potassium equilibrium potential or to shorten the action potential. Those channels can be classified on the basis of differences in their functional and pharmacological properties. Among the many potassium currents, distinction can be made between voltage-activated currents (Ito, IKur, IKr, and IKs), the inward rectifier currents (IK1, IKACh, IKATP) and two pore domain K^+ channels (see Table1).

K_2P currents in cardiomyocytes are insensitive to conventional K^+ channel blockers (4-AP, TEA, Ba^{2+}, Cs^+, glibenclamide). Several members of the K_2P family such as TREK-1 show high sensitivity to membrane stretch, changes in pH, fatty acids and inhalation (e.g. halothane, isoflurane, chloroform) and local (e.g. bupivacaine) anesthetic agents and are regulated by second messenger phosphorylation.

The following seven K_2P channels were detected in the mammalian heart, at low or high levels, by Northern and reverse transcriptase–polymerase chain reaction (RT-PCR) experiments: TWIK-1 (human), TWIK-2 (human and rat), TREK-1 (mouse), TASK-1 (human, mouse, and rat), TASK-3 (rat), THIK-1 (rat), and TALK-2 (human). Among those cardiac K_2P channels only two functional channels were recorded: TASK-1 and TREK-1. TREK-1 is one of the most attractive members in the K_2P channel family. It is activated by membrane stretch, by polyunsaturated fatty acids such as arachidonic acid, and by intracellular acidification.

Table 1. The potassium current of ventricular cardiomyocyte

Cardiac Current	Species	Protein	Gene	Open in action potential (phase)
Ito_f		Kv4.2	KCND2	1
		Kv4.3	KCND3	1
Itos		Kv1.4	KCNA4	1,2
$I_{K,slow}$	mouse	Kv2.1	KCNB1	1,2
		Kv1.5	KCNA5	1,2
	rat	Kv1.2	KCNA2	1,2
$I_{K,ur}$	human/rat /mouse	Kv1.5	KCNA5	1,2,3
$I_{K,ss}$	mouse	Kv2.1	KCNB1	1,2,3
	rat	Kv1.5	KCNK5	1,2,3
I_{Kr}		erg1	KCNH2	1,2,3
I_{Ks}		KvLQT1	KCNQ1	1,2,3
I_{K1}		Kir2.1	KCNJ2	0,1,2,3,4
		Kir2.2	KCNJ12	0,1,2,3,4
I_{KAch}		Kir3.1	KCNJ3	
		Kir3.4	KCNJ5	
I_{KATP}		Kir6.2	KCNJ11	0,1,2,3,4
I_{K2P}		TASK-1	KCNK3	0,1,2,3,4
		TREK-1	KCNK2	0,1,2,3,4

2.1 Cardiac TASK-1

The presence of TASK-1 mRNA in single rat ventricular and atrial cells has been confirmed by RT-PCR (Kim et al., 1998). Native TASK-1 channel currents with properties indistinguishable from cloned TASK-1 channel were first recorded by Kim (Kim et al., 1999). A 14-pS K^+ channel with kinetic properties similar to those of TASK-1 was identified in rat atrial and ventricular cells (Fig. 3) and it has a significant effect on the resting potential of atrium.

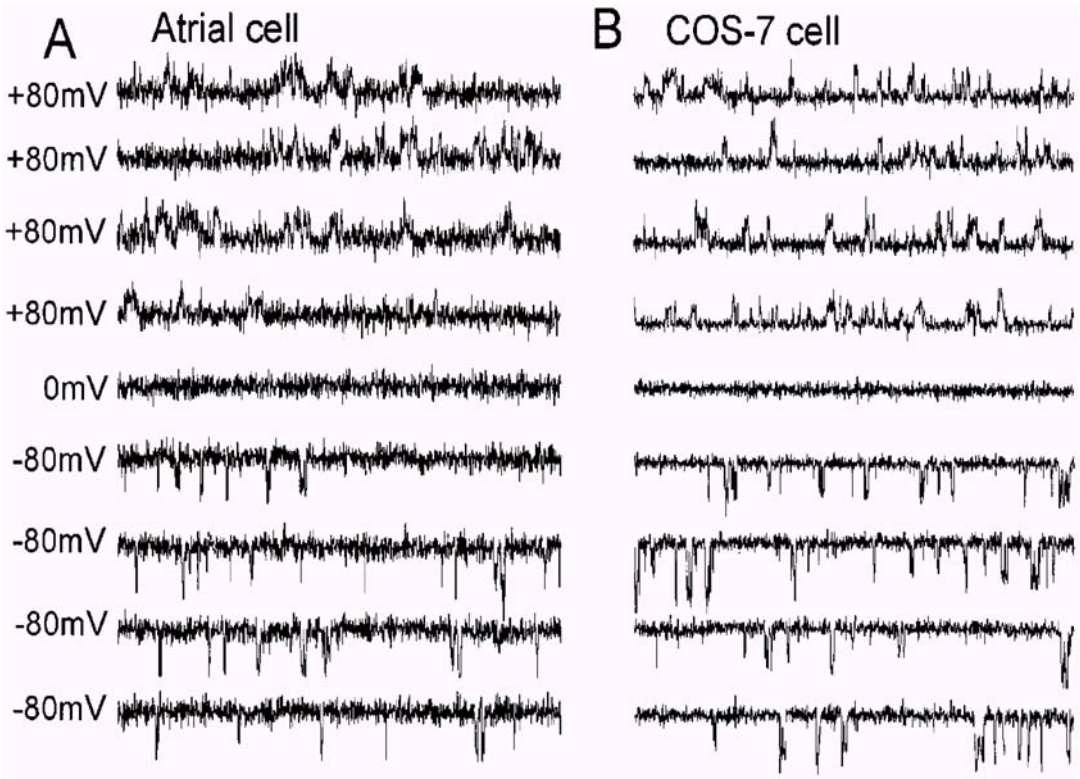

Figure 3. Identification of TASK-like K^+ channel in rat atrial cells
A, inside-out patch of TASK-like K^+ channel in a right atrial cell held at different potentials. B, inside-out patch of a COS-7 cell transfected with TBAK-1. Single-channel conductances were 13.5 pS at -80 mV and 9.6 pS at +80 mV for rat atrial K^+ channel (Kim et al., 1999).

2.2 Cardiac TREK-1

In initial studies, Kim et al. found arachidonic acid and intracellular acidosis activated a previously unknown K^+ channel in cardiac myocytes (Kim et al., 1989, 1990). Outwardly rectifying potassium-selective channels with conductances of 160 pS (IK_{AA}) can be opened by arachidonic acid in inside-out patches. The unknown

potassium channel was not sensitive to internally applied adenosine triphosphate (ATP), magnesium, or calcium. Lowering the intracellular pH from 7.2 to 6.8 or 6.4 reversibly increased the channel activity three or tenfold. The K^+ channel found by Kim may play an important role in protecting against cell damage caused by ischemia, which is known to elevate intracellular levels of certain fatty acids, including arachidonic acid (Schror et al., 1987).

Recently, a similar stretch-activated pH sensitive channel was also found in rat ventricular muscle (Tan et al., 2002). This channel displayed a nearly linear current-voltage relation with a slope conductance of 111 pS at +60 mV. The stretch activated TREK-1 like potassium channel was reversibly activated by clinical concentrations of volatile anesthetics. In cell attached experiments, the channel was inhibited by 500 μM chlorophenylthio-cAMP and also by stimulation of β-adrenergic receptors with 1 μM isoproterenol (Terrenoire et al., 2001).

Evidence for the expression of TREK-1 in atrial (Terrenoire et al*.,* 2001; Niu & Sachs, 2003) and cardiac ventricular myocytes (Aimond et al., 2000; Tan et al., 2002, 2004) has been obtained by RT-PCR.

3. Cardiac stretch activated ion channels: possible role in arrhythmogenesis

The electrical activity controls the mechanical activity of the heart. The time course and amplitude of the contraction of cardiac muscle depends on action potential duration, on frequency, and on the timing and pattern of preceding action potentials. Conversely, mechanical stimulation modulates the electrical activity of the heart in a complex manner, a phenomenon termed mechanoelectric feedback (Taggart et al., 1996; Ravens et al., 2003). Mechanical stimulation activates a variety of ion channels in cardiac muscle including stretch-activated non-selective cation channels (Kamkin et al., 2000; Zeng et al., 2000) and mechanosensitive potassium channels (Kim., 1992; Isenberg et al., 2003; Niu & Sachs., 2003). Mechanical stretch of isolated cardiomyocytes can give rise to changes in action potential configuration and to pacemaker-like afterdepolarizations (Kamkin et al., 2000; Isenberg et al., 2003;

Ravens., 2003). Mechanical stretch of isolated hearts can initiate premature beats or ventricular fibrillation (Franz et al., 1989). The arrhythmogenic effects of mechanoelectric feedback are of considerable pathophysiological interest (Ravens., 2003), but the physiological function of stretch-activated potassium channels in the heart is unknown.

3.1 Stretch-activated non-selective cation channels (SACs)

Application of longitudinal stretch in freshly isolated myocytes prolonged the duration of action potentials elicited by external stimulation, depolarized the resting membrane potential and initiated "spontaneous" action potentials.

Under whole cell configuration with 0mM K^+ bath and pipette solution, the amplitude of stretch induced transmembrane currents increased reversibly with the magnitude of stretch. The reversal potential of I_{SAC} is 0mV and is not sensitive to substitution of Cl^- with aspartate ions in the bath solutions. I_{SAC} was inhibited by 5μM gadolinium (Gd^{3+})(Kamkin et al., 2003). Thus, stretch-induced Na^+ influx is suggested to prolong APD90 and to promote late depolarization. As a consequence, intensity of I_{SAC} in myocytes from diseased human hearts may play important role in arrhythmia.

3.2 Stretch-activated potassium channels (SAKs)

Evidence suggested that there exists functional stretch-activated potassium channels (SAKs) in cardiomyocytes (Isenberg et al., 2003; Niu & Sachs., 2003). But from single channel levels, so far only a potassium channel was identified in heart by Kim (Kim, 1992): TREK-1. TREK-1 like potassium channels are not only activated by polyunsaturated fatty acid and intracellular acidosis but also by membrane stretch.

3.3 Anrep effect

Von Anrep found that when aortic resistance was elevated abruptly in the heart-lung preparation, the ventricular volume at first increased, but subsequently returned toward normal within 1 or 2 minutes because a positive inotropic effect followed (Von Anrep, 1912). Stretch of cardiac muscle generates a biphasic force response, with a rapid increase in force that has been attributed to increased myofilament Ca^{2+}

responsiveness and a second slowly developing phase, the SFR. SFR results from an increase in the Ca^{2+} transient. The SFR was the possible explanation for the Anrep effect (Tucci et al., 1984).

4. The objective of this study

In this thesis I will describe the biophysical characteristics and the possible functional role of cardiac mechano-gated TREK-like potassium channels in cardiac muscle. In addition I summarize the expression of TREK-1-like potassium channels in heart tissue, immunolocalization of K_2P channel in single cardiomyocytes and the properties of stretch-activated K^+ currents in heart. The latter objectives were met in collaboration with several colleagues whose contributions are appreciated: RT-PCR analysis of TREK-1 was carried out by Dr. Regina Preisig-Müller; immunohistochemistry of TREK-1 was done by Ms. Marylou Zuzarte; whole cell recording to identify I_{SAC} and I_{SAK} of heart was carried out by Vitaly Dyachenko from Julius-Bernstein-Institute for Physiology of the University of Halle and some whole-cell recording were contributed by Dr. Caroline Putzke from Klinikum of University of Marburg. These data are included in the result section of this thesis to provide a complete overview of the study.

Materials and methods

1. Cell isolation

Isolated cardiomyocytes was obtained from Wistar rat hearts by enzymatic dispersion. Wistar rats weighing 100–200g were decapitated and their hearts rapidly excised. A cannula was attached to the aorta (Langendorff preparation), and the coronary arteries were perfused at a constant flow rate of 10 ml/min using a peristaltic pump. The heart was submerged in a small organ bath warmed to 37°C.

The perfusing solution contained (in mM) 135 NaCl, 5 KCl, 1 $CaCl_2$, 1 $MgCl_2$, 0.33 NaH_2PO_4, 2 Na-pyruvate, 10 glucose, and 10 HEPES. The pH was 7.4 (adjusted with NaOH).

The temperature was 37°C and the elevated K^+ concentration of the perfusate caused cardiac arrest. To initiate dissociation of the cells, the heart was perfused for 5 min with nominally Ca^{2+}-free solution, which otherwise had the same composition as described above. The heart was then perfused for 10 min with Ca^{2+}-free solution to which 20 μM Ca^{2+} and 1 or 1.5 mg/ml collagenase (Worthington, type II) was added. Digestion of collagenase lasted 10-20 minutes. Subsequently, the heart was removed from the organ bath, washed briefly in a ‘‘storage solution’’ containing (in mM) 65 K-glutamate, 45 KCl, 30 KH_2PO_4, 3 $MgSO_4$, 0.5 EGTA, 20 taurine, and 10 glucose (pH adjusted to 7.4 with KOH), and submerged in 30 ml of storage solution. The heart was then cut into small pieces, and the cells were suspended by gentle trituration with a Pasteur pipette.

2. Patch-clamp recording of currents from rat cardiomyocytes

2.1 Single-channel and whole-cell recording

There are four basic different configurations of patch clamp (Fig. 4). The cell-attached patch mode produced by applying light suction to the patch pipette to produce a "gigaseal" ($\geq 10^9$ Ω). This mode is used to record the microscopic currents from only one channel or from a few channels. The whole-cell clamp mode is produced by applying strong suction to the patch pipette to rupture the membrane patch and allowing

the lumen of the pipette to be continuous with the lumen of the cell. This mode is used to record the macroscopic currents from all ion channels in the cell membrane. Withdrawal of the pipette from the membrane of cell-attached and whole-cell mode respective leads to two distinct cell-free recording configurations: inside-out and outside-out. Both modes are employed for recording the single channel currents (Hamill et al., 1981).

2.2 Definitions and conventions

1. Polarity of measured signals

The flow of positive current out of the head stage of the amplifier and out of the patch electrode generates a positive voltage signal at the output of the amplifier proportional to the measured current.

2. Inward current

Current that flows across the membrane, from the outside surface to inside surface, is termed inward current.

3. Outward current

Current that flows across the membrane, from the inside surface to outside surface, is termed outward current.

4. Positive potential

The term positive potential means a positive voltage at the headstage input with respect to ground.

5. Transmembrane potential

The transmembrane potential (Vm) is the potential at the inside of the cell minus the potential at the outside. The term is applied equally to the whole-cell membrane and to membrane patches.

6. Depolarizing/Hyperpolarizing

The resting Vm value of most cells is negative. If a positive current flows into the cell, Vm initially becomes less negative. Since the absolute magnitude of Vm is smaller, the current is said to depolarize the cell. Hyperpolarization is a negative shift in Vm.

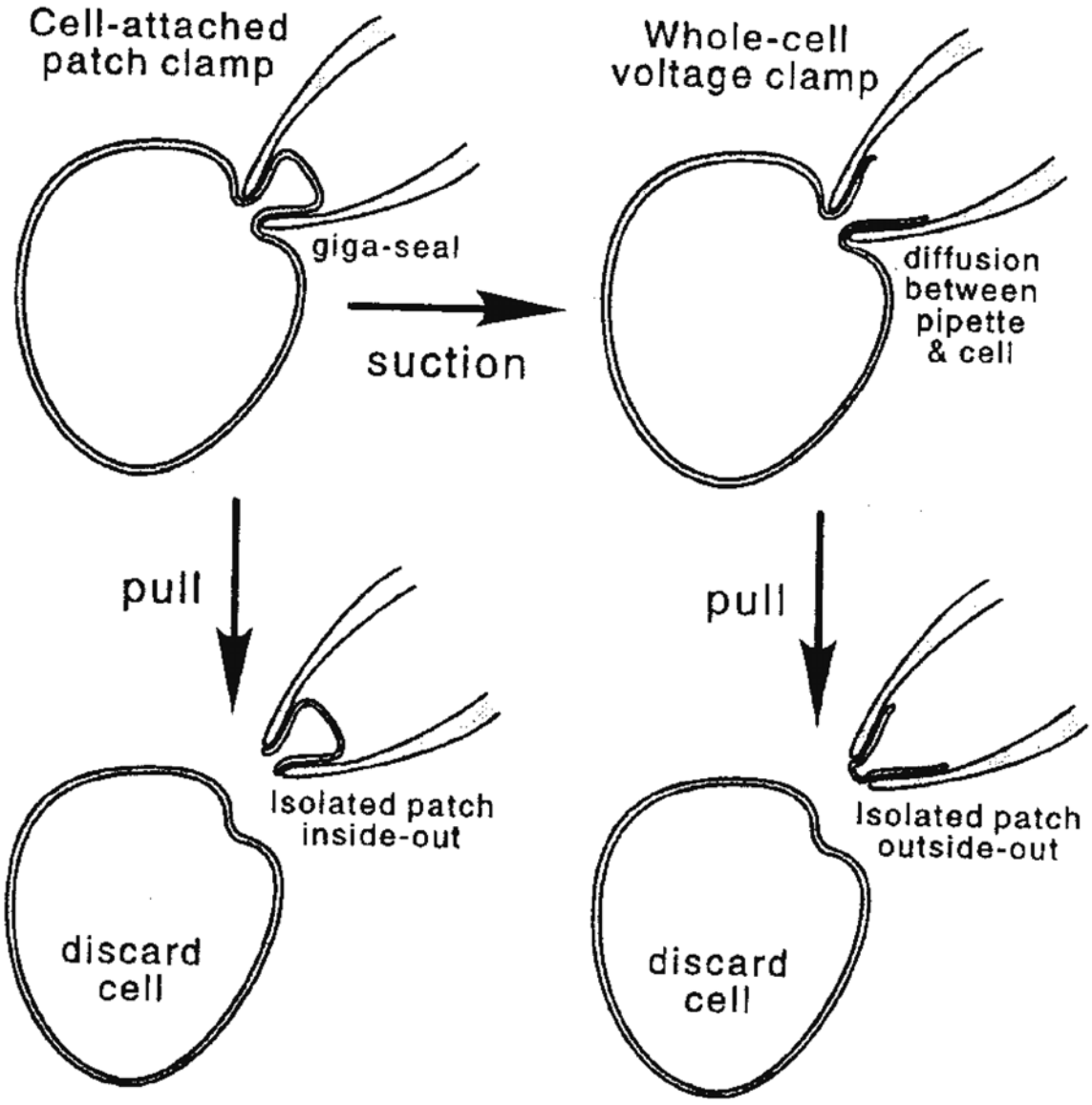

Figure 4. Schematic representation of the procedures which lead to recording configurations

The four recording configurations described in here are: "cell-attached". "whole-cell recording", "outside-out patch", and "inside-out patch". The upper left frame is the configuration of slight suction the seal between membrane and pipette increases in resistance by 2 to 3 orders of magnitude, forming what we call a cell-attached patch. The improved seal allows a l0-fold reduction in background noise. Upper right, voltage clamp currents from whole cell can be record after disruption of the patch membrane if cells of sufficiently small diameter are used. Bottom left, withdrawal of the pipette from the cell-attached (pull) and short exposure of the pipette tip to air can get isolated inside-out patch. Bottom right, after withdrawal of the pipette from the whole-cell mode (pull) it is outside-out patch (Hamil et al., 1981).

2.3 Single channel analysis

Events

For single channel analysis, an event is defined as a sudden change in current as the result of opening or closing of an ion channel.

Single-channel current amplitude

Amplitude histograms can be used to define the conductance of states of single channels. Two kinds of amplitude histograms are common: point histograms and event histograms. The former use all the acquired data points and the latter use each event in the event list.

Dwell time

A patch clamp record of activity of a single channel will show a sequence of alternate open and shut periods of different duration, the duration of any particular open or closed events is its dwell time, denoted by t. A common method of analyzing single channel records is to sort the individual events according to their dwell times, putting them into a series of bins of constant width. After several hundred or more openings have been sorted in this way, normally by computer, a dwell time histogram for the open state of the channel will be produced. A similar procedure is used to produce a closed state histogram. These histograms can usually be fitted by one or more exponential function.

The open probability: Po

The fraction of time that an ion channel is open during a recording is represented symbolically as Po, the probability that a channel is open. Po can be calculated as the fraction of data samples that fall into the open channel current distribution from raw data histogram.

2.4 Whole-cell recording configuration

Electrical circuit of Whole cell recording

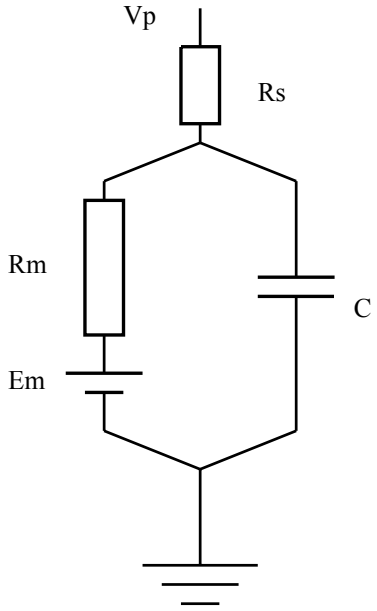

This is the electrical circuit of whole cell recording. Rm is membrane resistance and Rs represents the series resistance. Em is the resting membrane potential of cells. C means capacitance that depends on cell size. Vp is pipette potential.

The resting membrane potential

Most cells possess a resting membrane potential, a voltage across the plasma membrane such that the inside is usually some tens of millivolts negative to outside in the resting condition. The resting membrane potential is often close to the potassium equilibrium, indicating that under resting conditions, the permeability to K^+ is dominant over other permeability.

Series resistance

Series resistance (Rs) is a resistance in series with the membrane. Part of the series resistance arises from the pipette itself, but normally the major part arises from the residual resistance of broken patch membrane, which provides the electrical access to

the cell interior. In practice, the series resistance usually can not be reduced below a value about two times the resistance of the pipette alone.

2.5 Single and whole recording in rat ventricular cells

Cardiomyocytes of Wistar rat were isolated as described above. Drops of the cell suspension were transferred to a small recording chamber that was mounted on the stage of an inverted microscope (Ziss Axiovert 35). Single channel currents were recorded using an Axopatch 200B patch clamp amplifier (Axon instruments, USA). The pipette resistance was in the range 8–12 MΩ.

The pipette and bath solution used for cardiomyocytes contained (mM): 140 KCl, 1 $MgCl_2$, 5 EGTA and 10 HEPES (pH, 7.3). The data were acquired with PC DAQ1.1.5 software and analysed with software developed in our laboratory using LabView (National Instruments). Single-channel currents were sampled at 10 kHz and filtered with a -3 dB cutoff frequency of 2 kHz.

Whole-cell clamp experiments in cardiomyocytes before and after application of arachidonic acid were performed as described previously (Liu et al., 2001b). For whole-cell recordings during mechanical stretch, myocytes were prepared according to Isenberg & Klöckner (1982). The bath solution contained (mM) 150 NaCl, 5.4 KCl, 1.2 $MgCl_2$, 20 glucose, 10 HEPES/NaOH (pH, 7.4) and the pipette solution contained (mM) 140 KCl, 5 EGTA, 5.5 $MgCl_2$, 5 Na_2ATP, 10 MOPS, adjusted to pH 6.0. Whole-cell currents were recorded with an RK-300 amplifier (Biologic, Echirolle, France). The data were filtered at 2 kHz, sampled at 5 kHz and digitized with the CED1401 interface (Cambridge instruments, Cambridge, UK). Voltage-clamp commands and mechanical stretch were controlled by custom-written software. The isolated cardiomyocytes were continuously stimulated with 35 ms pulses from –45 to 0 mV at a rate of 1 Hz. The input resistance at 0 mV was >0.4 GΩ; the mean capacitance was 196±22 pF. To study the effect of cell deformation on the net membrane currents, the membrane was clamped to +60 mV for 50 ms and then repolarized from +60 to -100 mV at a rate of -200 mV s^{-1}. Curve fit and data evaluation were performed as described previously (Isenberg et al., 2003).

Mechanical stimulation was performed with a glass stylus (Kamkin et al., 2000) pulled from thick walled borosilicate glass capillaries of 2 mm outer diameter. The end of the stylus was fire-polished to a semi-sphere with a diameter of ≈20 µm. Patch pipette and stylus were mounted on two piezo-driven micromanipulators (Burleigh PCS-5000, Victor, NY) equipped with an analog input (npi, Heidelberg, Germany) for control of x and z axis positions. The distance between stylus and patch pipette was increased with a time constant of 20 ms. The extent of the movement (µm per mV analog input) was calibrated in the microscope setup. Before attachment, stylus and patch electrode were separated by ≈50 µm (48±2 µm, n=41). In typical stretch experiments this distance was increased to 55 µm.

3. Recording of TREK-1a and TREK-1b channels expressed in HEK293 and COS-7 cells

3.1 Cell culture

HEK293 cells and COS-7 cells were grown in Dulbecco's modified Eagle's medium (DMEM, life Technologies) in Flask. For subculturing, the culture medium was removed and discarded and briefly rinsed the cell layer with 0.25% (w/v) Trypsin-0.53 mM EDTA solution to remove all traces of serum that contains trypsin inhibitor. Add 2.0 to 3.0 ml of Trypsin-EDTA solution to flask and observe cells under an inverted microscope until cell layer is dispersed (usually within 5 to 15 minutes). The next step is putting 6.0 ml complete growth medium and aspirate cells by gently pipetting. The appropriate aliquots of the cell suspension were put to new culture vessels. Finally HEK293 cells and COS-7 cells were grown in 35mm tissue culture dishes.

3.2 Transfection

After 24 hours growth cells reached a density of ~2 $\times 10^5$/35-mm dish and were transfected with 0.6–1 µg of rTREK-1 in the pcDNA3.1(1) vector, using LipofectAMINE (Life Technologies, Inc.).

At first, the DNA was diluted in 50 µl of Opti-MEM I Reduced Serum Medium without serum (or other medium without serum) and mixed gently. Lipofectamine™ 2000 was mixed gently before use then diluted the appropriate amount in 50 µl of Opti-MEM I Medium. After incubated for 5 minutes at room temperature, the diluted Lipofectamine™ 2000 and diluted DNA were combined (total volume = 100 µl) within 30 minutes and incubated for 20 minutes at room temperature. The 100µl of complexes were put into each dish containing cells and medium and mixed gently by rocking the plate back and forth. Then the cells were incubated in a CO_2 incubator for 18-48 hours prior to testing for transgene expression. It is not necessary to change the medium, but medium may be replaced after 4-6 hours.

3.3 Electrophysiological recording

Inside-out and cell-attached single channel currents were recorded using an Axopatch 200B patch clamp amplifier (Axon instruments, Union City, CA, USA) within 24-48 hours after transfection. The pipette resistance was in the range of 8–12 MΩ. The normal pipette and bath solution contained: 140 mM KCl, 1 mM $MgCl_2$, 5 mM EGTA, 10 mM HEPES; the pH was adjusted to 7.3 with KOH. Single-channel currents were sampled at 10 kHz and filtered with a -3 dB cutoff frequency of 2 kHz.
All experiments with cardiomyocytes or transfected cells were carried out at room temperature (22 ^{o}C).

4. Drugs

Salts and other chemicals were purchased from Sigma (St. Louis, MO, USA). 4-aminopyridine (4-AP), tetraethylammonium (TEA), Ba^{2+}, cadmium (Cd^{2+}) and bupivacaine were directly dissolved in bath solutions.

Arachidonic acid was obtained from Sigma and dissolved in ethanol to make up a 10 mM stock solution and kept at -25 ^{o}C. The small volumes of the stock solution were added and vortexed 2 minutes to produce the desired final concentration in the superfusate. The final ethanol concentration in the superfusate was always less than 0.01% and had no electrophysiological effects at this concentration. Glibenclamide was dissolved in dimethylsulphoxide (DMSO) and make up to the 10 mM stock solution.

Glibenclamide was added to the bath solution and get a final concentration of 2 μM. A 10 mM stock solution of forskolin also was dissolved in the bath solution and the applied concentration was 10 μM. The final DMSO concentration in the bath solution was less than 0.1% and had no electrophysiological effects at the ion channels studied.

5. Immunofluorescence microscopy

Glass cover slips were acid washed over night and washed thoroughly with distilled water before sterilizing in EtOH. The cover slips dried under the sterile hood before being stored in a dry Petri dish. Freshly isolated myocytes were allowed to settle and attach on acid-washed cover slips for 30 minutes. The cells were then washed with PBS and fixed with 4% PFA for 15 minutes at room temperature. Following three washes with PBS the cells were permeabilized with 0.2% Triton-X100 for 10 minutes. The cells were washed three times by PBS and then blocked with 1% BSA (Fraction IV, Sigma) and 5% horse serum (Vector Labs) for 30 minutes at room temperature.

The primary antibody for TASK-1 was from Alomone. The primary antibody for TREK-1, which should detect both splice variants of the channel protein, was from Santa Cruz (TREK-1-E-19). The dilution used for the primary antibodies was 1:100. The myocytes were incubated with the primary antibody for 1 hour at room temperature, which cover in humidified chamber to prevent drying antibody. After this, myocytes were washed by PBS buffer for three times.

The Alexa donkey anti-mouse Fluor 488 and 594 were from Molecular Probes and employed as secondary antibodies at a dilution of 1:1000. The second antibody containing fluorescence tag was added and incubated for 5 minutes. PBS washed the myocytes for three times. The cover slips were embedded onto glass slides using a drop of Mowiol containing n-Propyll gallate. The samples of cover slips allowed drying before imaging and analyzing.

Wide field images of cardiomyocytes stained for either TASK-1 or TREK-1 were obtained on an inverted microscope (Olympus IX70) equipped with a 60× objective (numerical aperture, 1.45) and a digital camera (PCO SensiCam, QE). Confocal images from 15 cardiomyocytes co-stained for TASK-1 and TREK-1 were

obtained with a Zeiss LSM 510 Meta. Z-stacks were acquired at distances between 300 and 560 nm.

As a check for the specificity of the TREK-1 antibodies, COS-7 cells, cultured on cover slips, were transfected with TREK-1a as described above for HEK293 cells. 48 hours after transfection, COS-7 cells were prepared for microscopy by the same procedure as described above for cardiomyocytes.

6. RNA extraction

Isolation of cardiomyocytes and expression analysis of RNA from pure cardiomyocytes was performed as described previously (Preisig-Muller et al., 1999). Total RNA from isolated cardiomyocytes was extracted by using the Highpure RNA kit (Roche, Mannheim, Germany), which included DNase I digestion. Usually about 500 cardiomyocytes were picked under visual control by using a hydraulic cell picker and transferred to 500 µl of the lysis buffer. Subsequently, total RNA was extracted according to the instructions of the manufacturer and eluted into 50µl RNase-free water.

7. Reverse transcription

Reverse transcription (RT) was performed by using 200 units Superscript II reverse transcriptase (Invitrogen) and a random hexanucleotide (Applied Biosystems)

RT reaction (20 µl)	
RNA (1µg)	10µl
5 × RT Buffer	5 µl
10 × random hexanucleotides	0.5µl
dNTP (2 mM)	6 µl
DTT (0.1 µM)	2.5µl
Superscript II (200U/µl)	1 µl

mixture. In a 20µl RT reaction either 10µl eluate of total RNA extracted from pure rat cardiomyocytes or 1µg of total rat heart RNA (purchased from Clontech) were used.

The RT reaction was incubated for 50 minutes at 42°C and finally the Superscript II reverse transcriptase was inactivated by heating at 70°C for 15 minutes.

8. Cell-specific RT-PCR

Cell-specific RT-PCR expression analysis was performed with gene-specific, intron-spanning primers of 24–28 nucleotides in length. The total PCR volume was 25 µl, including 1-2 µl of RT reaction, 25 pmol of each primer, and 1.2 units of AmpliTaq Gold (Applied Biosystems). The tubes were placed in the thermal cycler (model 2400, Applied Biosystems). Following is the volume of composition:

PCR reaction (25 µl)	
10×PCR Buffer + 15mM $MgCl_2$	2.5 µl
DMSO	1 µl
dNTP (2 mM)	2.5 µl
Forward primer (25 pmol/µl)	1 µl
Reverse primer (25 pmol/µl)	1 µl
Taq DNA polymerase (5 U/µl)	0.24 µl
cDNA from first-strand reaction	1 µl
RNase-DNase free water	15.76 µl

PCR was run with a hot start for 5 min at 96°C; then for 35 cycles of 0.5 min at 96°C, 0.5 min at 55°C, and 1.5 min at 72°C; and finally 10 min at 72°C (final extension).

15 µl of the PCR probe were size fractionated by agarose gel electrophoresis. To verify the identity of the PCR products, DNA fragments of the expected length were isolated and directly sequenced using an ABI prism 310 DNAsequencer (Applied Biosystems).

The RT-PCR expression analysis was performed with gene-specific and intron-spanning primers for GAPDH (house-keeping gene) and TREK-1 splice forms. To verify the isolation of pure cardiomyocytes we used the following marker genes: troponin T (TnT) for cardiomyocytes, endothelin-1 for endothelial cells and calponin-1 for smooth muscle cells. The following primers were used:

GAPDH (343 bp fragment): for 5′-CATCACCATCTT CCAGGAGCGA-3′, rev 5′-GTCTTCTGGGTGGCAGTGATGG-3′;

rTREK1 (398 bp fragment): for 5′-CTCAGGAGATTTCTCAGAGGACCAC-3′, rev 5′-CTAACATTCCACTTAATAAATGT GTC-3′;

rTREK1a (236 bp fragment): for 5′-CTGCCCGTGCAGCTCGGAGCG-3′, rev 5′-ACACCGTGGCTCCGATGATCAGGTA-3′;

rTREK1b (254 bp fragment): for 5′-GAATGCTGCATGCCTCATGCTT-3′, rev see above;

rTnT (525 bp fragment): for 5′-CTGAACGAGCTGCAGACTCTGATCG-3′, rev 5′-GACTTTCTGGTTGTCG TTGATCCTG-3′;

Endothelin-1 (360 bp fragment): for 5′-CGCAGGTCCAAGCGTTGCTCCTG CTC-3′, rev 5′-GTCTTGATGCTGTTGCTGATGGCCTC-3′;

Calponin (384 bp fragment): for 5′-GAGCCTGAGAAGCTGAGAGAAGGC-3′, rev 5′-CTCTGGATATTCCGGGGTCAGGCA-3′.

9. Gel extraction.

The DNA of a RT-PCR reaction was loaded on a 1.5% gel after mixing with the loading buffer. The electrophoresis was carried out in 1×TEA buffer at 80V for 30 min. The DNA fragments on the gel were stained with ethidiumbromide and fragments of the expected size were extracted by using a commercially available extraction kit according to the instructions of manufacturer (QIAquick gel extraction kit, Qiagen). Finally DNA was collected by eluting into 25-50 DNase/RNase-free water.

10. DNA restriction, ligation reactions, transformation into *Escherichia-coli* and isolation of Plasmid DNA

Restrication digestion was carried out at 37°C for 1-2 hours with the appropriate restriction enzymes. Ligation reactions were performed with T4-DNA ligase (New England Biolabs) at 16°C overnight. Ligated DNA was transformed into *Escherichia-coli* and plated onto LB plates containing the appropriate antibiotic. Recombinant plasmid DNA was isolated according to Qiagen handbook.

11. Statistics

Data are reported as means ± standard deviation. Unless otherwise stated, the statistical significance was evaluated by student's t-test. Difference were considered significant at $P<0.05$.

Results

1. Expression of TREK-1 channels in cardiomyocytes

The potassium channel TREK-1 (KCNK2) has at least two splice variants differing in exon 1 at their extreme N-terminus. The gene structure of both human and rat TREK-1 is shown in Fig. 5A. The channel sequence originally described for the mouse (Fink et al., 1996) is denoted TREK-1a here. TREK-1a from rat (accession number AY727922) differs from its mouse ortholog in only six amino acids. In all orthologs of TREK-1a, exon 1 encodes only a methionine residue. In the other splice variant, denoted TREK-1b here, exon 1 encodes 16 amino acids (Koizumi et al., 1999; Bockenhauer et al., 2001) (Fig. 5B and C). Both splice variants of TREK-1 are expressed in rat heart (Fig. 6A), whereas the other stretch-sensitive K_{2P} channels, TREK-2 and TRAAK, could not be detected with specific primers (not illustrated). Using cell-specific expression analysis we found robust expression of TREK-1b in rat cardiomyocytes (Fig. 6B). Re-amplification of the PCR-products showed that TREK-1a is also expressed in cardiomyocytes, albeit very weakly.

2. TREK-1 localization

Immunohistochemistry with antibodies against TREK-1 showed a striking localization pattern. The wide field image of TREK-1 proteins shown in Fig. 7A, focused on the surface of a rat cardiomyocyte, revealed distinct longitudinal stripes. In contrast, immunostaining of TASK-1, focused on the center of the cell, showed transverse stripes related to the T-tubules (Fig. 7B), as has been reported previously (Jones et al., 2002). The specificity of the TREK-1 antibody was checked by transfecting COS-7 cells with TREK-1a 48 hours before fixation. Fig. 7C shows TREK-1 positive transfected cells; no staining was seen in non-transfected cells (Fig. 7D). After pre-absorption with the antigenic peptide only very weak punctuate staining was observed (Fig. 7E). The secondary antibody conjugated with Alexa 488 showed no unspecific staining (Fig. 7F).

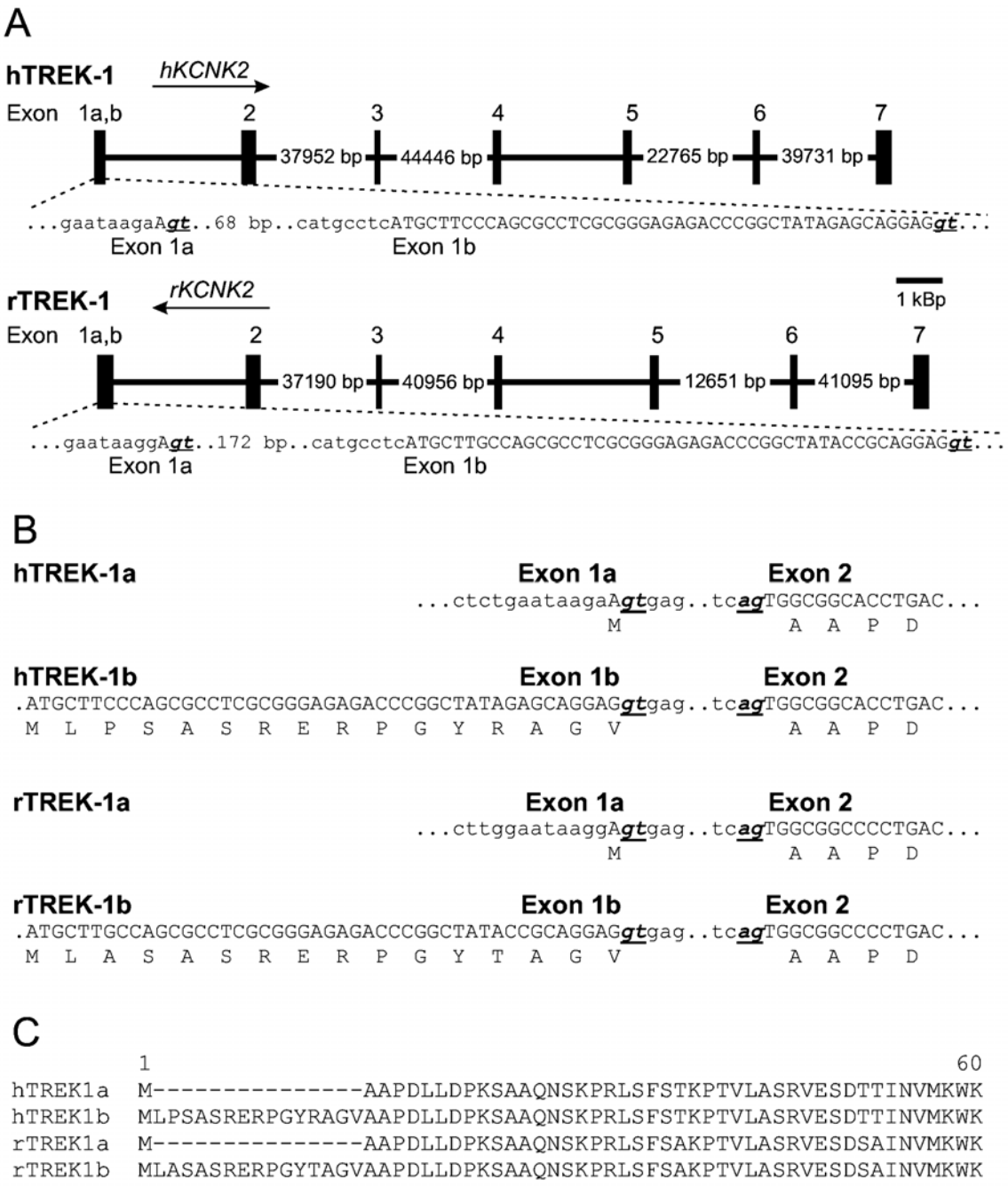

Figure 5. Gene structure of TREK-1 in cardiac muscle

A, gene structure of hTREK-1 and rTREK-1 and the nucleotide sequences of the two variants of exon 1 (Exon 1a and Exon 1b). hTREK-1 is on contig NT_021877.15, chromosome 1q41; rTREK-1 is on contig NW_042862.1, chromosome 13q26. B, N-terminal cDNA and amino acid sequences of human and rat TREK-1 splice variants. The accession numbers are AF004711 for hTREK-1b and AF325671 as well as AF385402 for rTREK-1b. The splice sites of the first intron are underlined and bold, the coding sequences are given in capital letters. C, alignment of the N-terminal region of the splice forms of human and rat TREK-1.

Confocal imaging of cardiomyocytes co-stained for TREK-1 and TASK-1 channel proteins (n=15) demonstrated that the longitudinal stripes of TREK-1 channels were restricted to the cell surface membrane, as illustrated in Fig. 8. In the T-tubules TASK-1 channels were prominent, but a weak TREK-1 signal could also be detected.

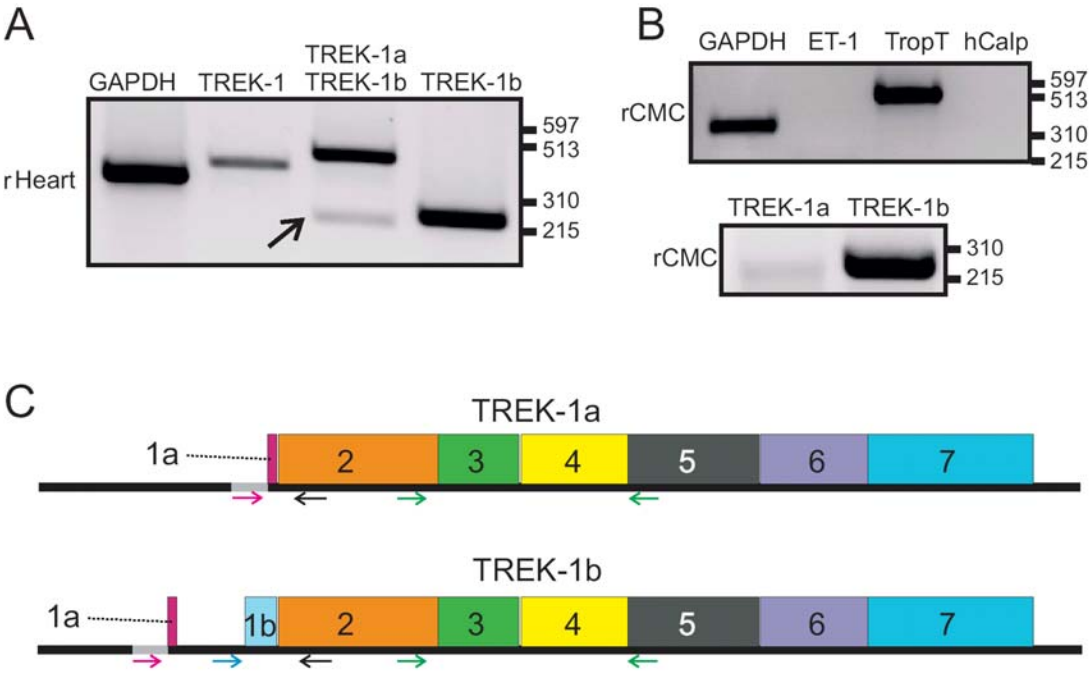

Figure 6. RT-PCR analysis of TREK-1a and TREK-1b
A, RT-PCR from rat (rHeart) heart tissue with three different primer pairs, recognizing all TREK-1 splice variants (TREK-1), TREK-1a and TREK-1b (giving two bands), or TREK-1b only (see text). GAPDH was used as housekeeping gene. B, cell-specific RT-PCR of rat cardiomyocytes (rCMC), performed as described previously (Preisig-Muller et al., 1999). Troponin T (TropT) was used as a marker for cardiomyocytes, rat endothelin-1 (ET-1) for endothelial cells and calponin-1 (hCalp) for vascular smooth muscle cells. The endothelin-1 and calponin-1 signals were negative in all myocyte preparations tested (n=5). Robust expression of TREK-1b was detected using 35 PCR cycles. Re-amplification showed very weak expression of TREK-1a as well. C, schematic drawing of the mRNA of TREK-1a and TREK-1b. The primer pair recognizing all splice variants (denoted TREK-1 in A) is indicated by green arrows. The forward primers for TREK-1a (red) and TREK-1b (blue) were used in combination with the same reverse primer (black). Note that, for clarity, the length of the exons is not exactly drawn to scale.

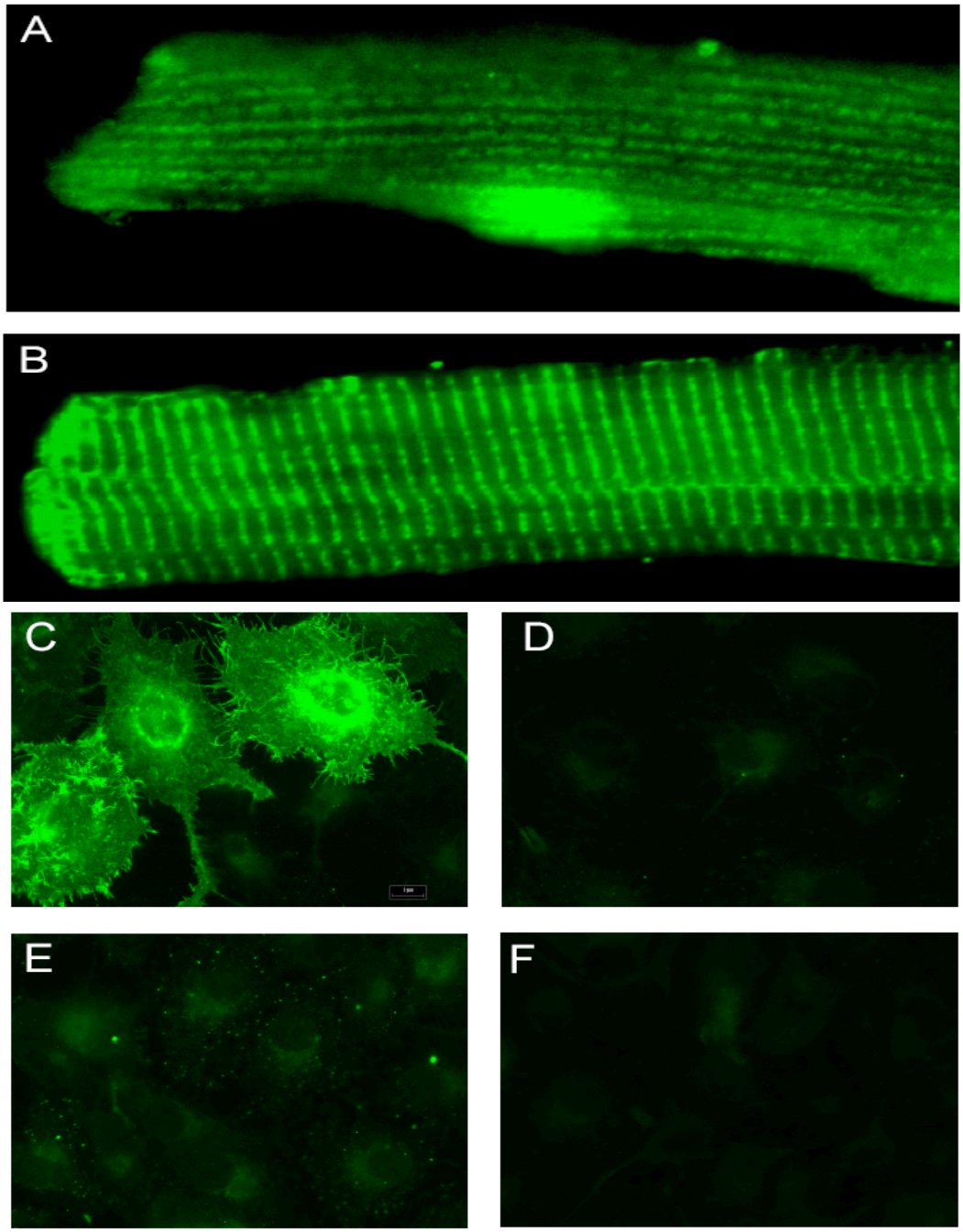

Figure 7. Immunofluorescence microscopy of TREK-1 and TASK-1 channels
A, immunostaining for TREK-1 proteins; the image was focused on the surface of the cell. B, immunostaining for TASK-1 proteins; the image was focused on the center of the cell. C-F, tests for the specificity of the TREK-1 antibodies. COS-7 cells were immunostained 48 hours after transfection with TREK-1a (C) or at the same time point without transfection (D). E, control image taken after preabsorption of the antibodies with the antigenic peptide supplied by the manufacturer. F, control image taken only with the secondary antibody.

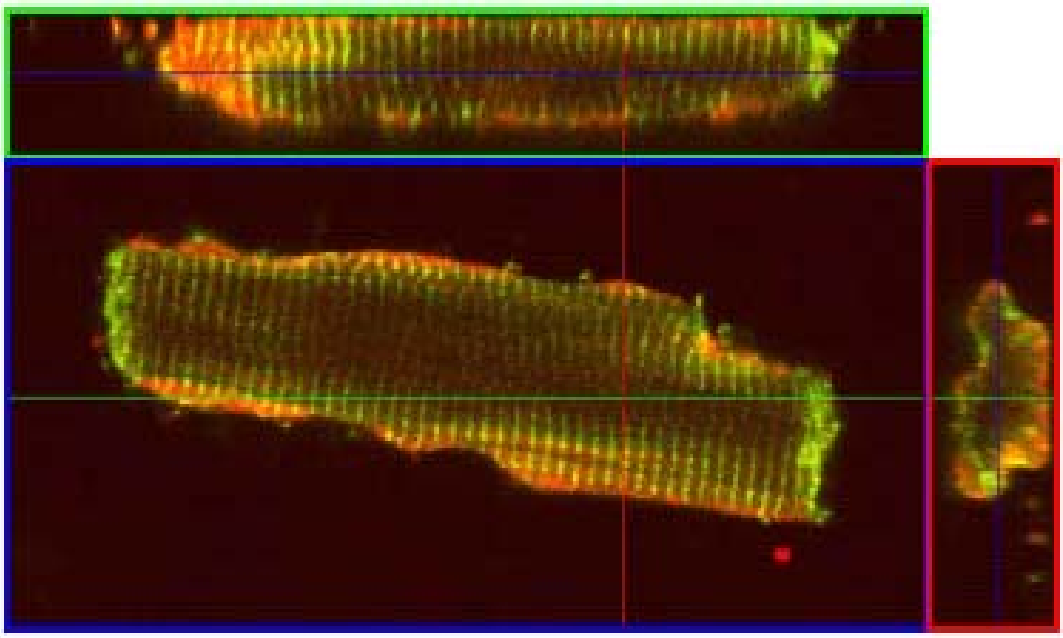

Figure 8. Subcellular localization of TREK-1 and TASK-1 in cardiomyocytes
Confocal image of a rat cardiomyocyte co-stained for TREK-1 (red) and TASK-1 (green). One XY, XZ and YZ plane is shown.

3. Changes in whole-cell current induced by arachidonic acid and axial stretch

Functional expression of the channels was tested by measuring the effect of arachidonic acid, a known activator of TREK-1 (Patel et al., 2001; Kim., 2003), on the steady-state current-voltage relation of rat ventricular cardiomyocytes. To eliminate any contribution of ATP-sensitive K^+ channels and voltage-activated Ca^{2+} channels, the measurements were carried out in the presence of 1 µM glibenclamide and 100 µM $CdCl_2$. Application of 10 µM arachidonic acid induced an additional steady-state out-

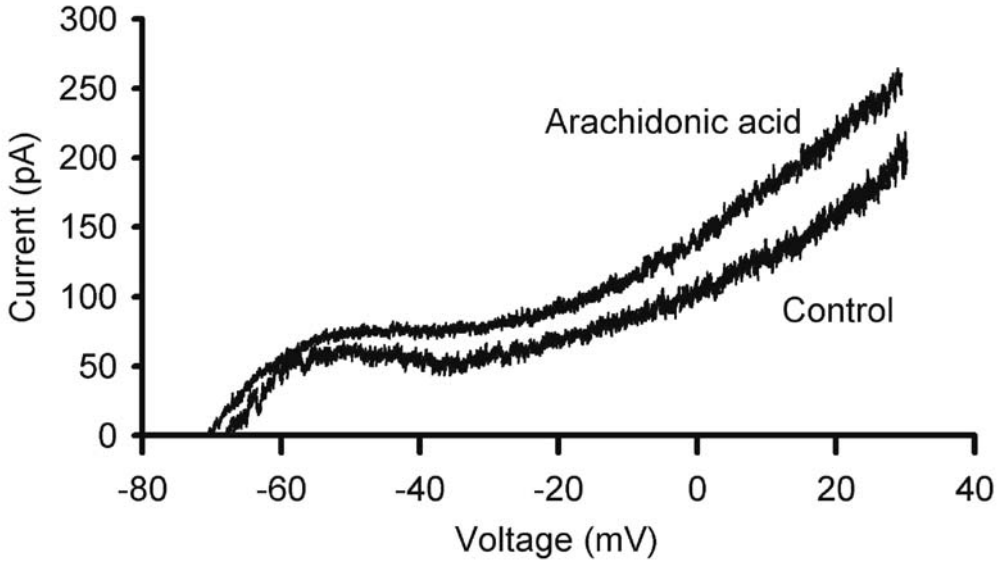

Figure 9. Effect of arachidonic acid on the current voltage relation in rat cardiomyocytes
Very slow voltage ramps (6 mV s^{-1}) were applied between +30 and -90 mV; the upper curve was obtained 10 min after application of 10 µM arachidonic acid.

ward current between -60 and +30 mV that increased with depolarization (Fig. 9). The difference current measured after application of 10µM arachidonic acid reversed near the calculated K^+ equilibrium potential and showed outward rectification. Under control conditions the current measured at +30 mV was 164±44 pA; 10 min after application of arachidonic acid it was 266±46 pA. Since the other two arachidonic-acid sensitive K_2P channels, TREK-2 and TRAAK, are not expressed in rat heart our findings suggest that

TREK-1 channels can carry a substantial current component in the plateau range of potentials.

Another important characteristic of TREK-1 is activation by membrane stretch. Therefore we studied the changes in whole-cell current induced by local axial stretch of cardiomyocytes. Previous studies in mouse and guinea-pig cardiomyocytes had shown that axial stretch changed several current components including stretch-activated nonselective cation channels (SACs), stretch-activated K^+ channels (SAKs) and inward rectifier channels (Kamkin et al., 2000; Isenberg et al., 2003). We have now confirmed these findings for rat cardiomyocytes (not illustrated). The stretch-activated current at positive potentials could be described by two components: a linear stretch-activated nonselective cation current with a reversal potential of ≈-10 mV (Kamkin et al., 2000; Niu & Sachs., 2003) and an outwardly rectifying stretch-activated K^+ current. Application of 5 µm stretch increased the outward current +60 mV from 950±283 to 1542±496 pA (n=10).

To study the stretch-activated K^+ current in more detail, we carried out whole-cell measurements in the presence of a blocker cocktail. L-type I_{Ca} and Na^+/Ca^{2+} exchange currents were eliminated by removal of extracellular Ca^{2+} and addition of 200 µM $CdCl_2$ to the bath solution; inward rectifier currents were minimized by addition of 500 µM $BaCl_2$; ATP-sensitive K^+ channels were blocked by 2 µM glibenclamide, β-adrenergic receptors (which might inhibit TREK-1 channels via PKA (Terrenoire et al., 2001)) were blocked by addition of 1 µM propranolol. We also tried to eliminate stretch-activated cation channels (SACs) with gadolinium, but application of 20 µM $GdCl_3$ blocked the mechanosensitivity of the K^+ current components as well. Since outward currents through SACs may superimpose on mechanosensitive K^+ currents we selected those experiments for analysis in which stretch produced only a small difference current at the K^+ equilibrium potential (<50 pA between -87 and -91 mV).

Fig. 10A shows a representative example of the outward currents recorded in the presence of the blocker cocktail. Application of stretch, i.e. increasing the distance

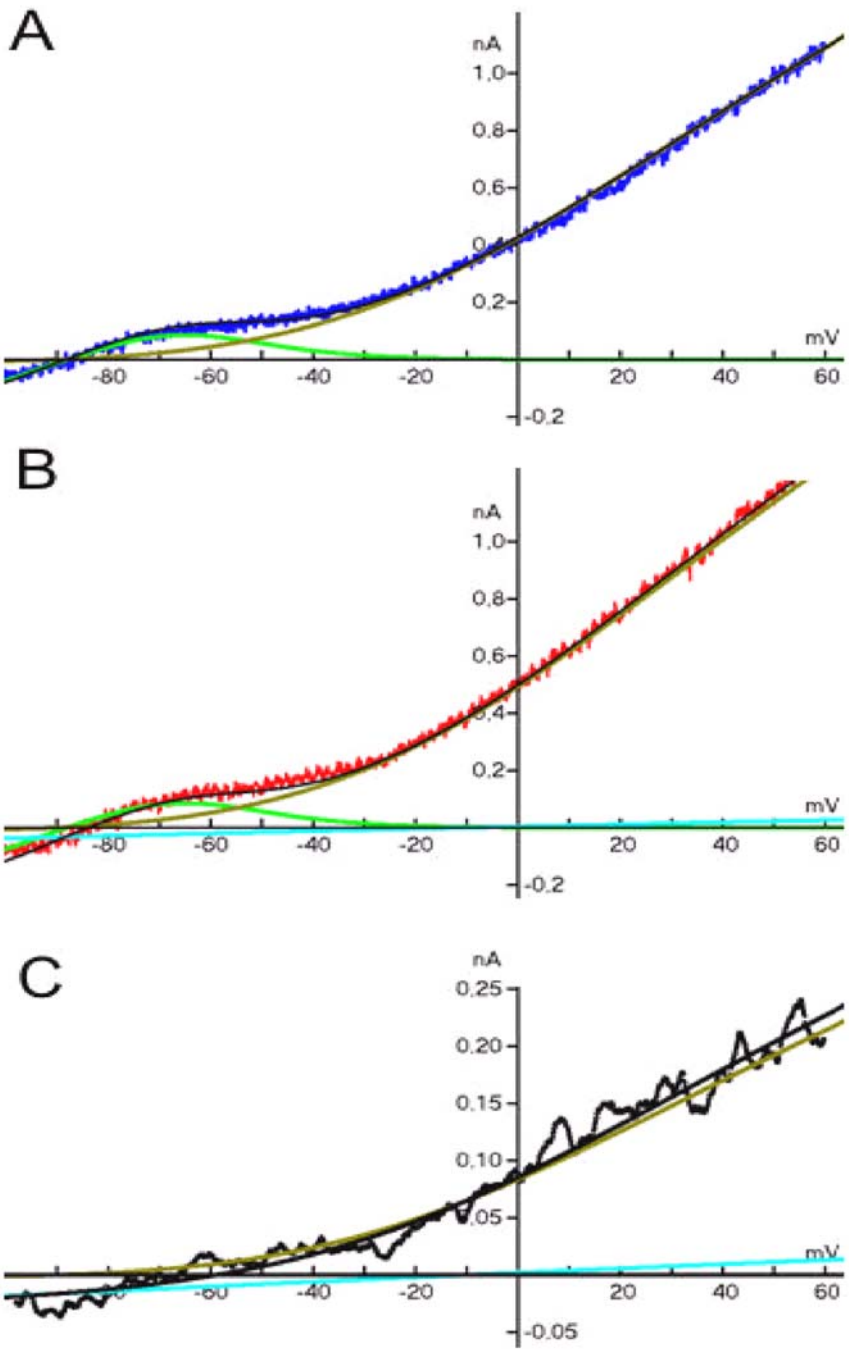

Figure 10. Effects of axial stretch on whole cell current in cardiomyocytes
Typical recordings in the presence of a blocker cocktail are shown (see text). The noisy lines represent the measured curves, the smooth lines represent the reconstructed curves. Current-voltage relations measured before (A, blue) and after stretch (B, red) were reconstructed (black) by adjusting the amplitude of the linear stretch-activated nonspecific cation current (light blue), a stretch-activated outwardly rectifying current (olive), and the residual inward rectifier component (green), as described in detail by Isenberg et al (2003). C, the measured difference current (noisy line) between A and B and the reconstructed difference current (black line).

between stylus and patch pipette by 5 µm, increased the stretch-activated K^+ current at +60 mV (olive line in Fig. 10B) by ≈200 pA. On average, 5 µm stretch increased the current at +60 mV from 1120±90 to 1320±40 pA (n=5). This increment in outward current was much larger than the calculated linear current component related to opening of SACs (light blue line). The voltage dependence of the difference current (Fig. 10C) showed outward rectification.

4. Native TREK-like K^+ channels in rat cardiomyocytes

To get more information on the elementary events underlying the stretch-activated K^+ current we then turned to single-channel recording. In outside-out patches from ventricular myocytes we found two K^+ channels that could be activated by stretch of the patch membrane and displayed the 'flickery burst' behavior typical for members of the K_{2P} family: bursts of brief openings interrupted by extremely short closures, and relatively long closures in between bursts (Fig. 11A and B). Typical all-point histograms (raw data) of the two channels measured in outside-out patches at -40 mV are shown in Fig. 11C and D.

The channel with the larger conductance (Fig. 11B), which was found in ≈15% of outside-out patches, showed outward rectification and had a conductance of 132.3±5.1 pS (n=4) at positive potentials (Fig. 11F, ■). Its biophysical properties were similar to those of the 'classical' TREK-1 channel (Kim & Duff., 1990; Kim., 1992; Terrenoire et al., 2001; Tan et al., 2002) and were therefore not studied further. The channel with the smaller conductance (Fig. 11A) has not been described previously in cardiac muscle. It showed slight inward rectification and had a conductance of 41.4±4.8 pS (n=10) at positive potentials (Fig. 11E, ■). This channel appears to be strongly expressed at the surface membrane since it was found in ≈60% of outside-out patches. The filled circles in Fig. 11E and F show the single-channel current voltage relations measured after reduction of extracellular K^+ from 140 to 32 mM. The extrapolated reversal potential (×) of both channels was shifted by about -34 mV, as predicted by the Nernst equation, indicating that the channels were indeed K^+ selective. The conductance of both TREK-like channels depended on the presence of extracellular

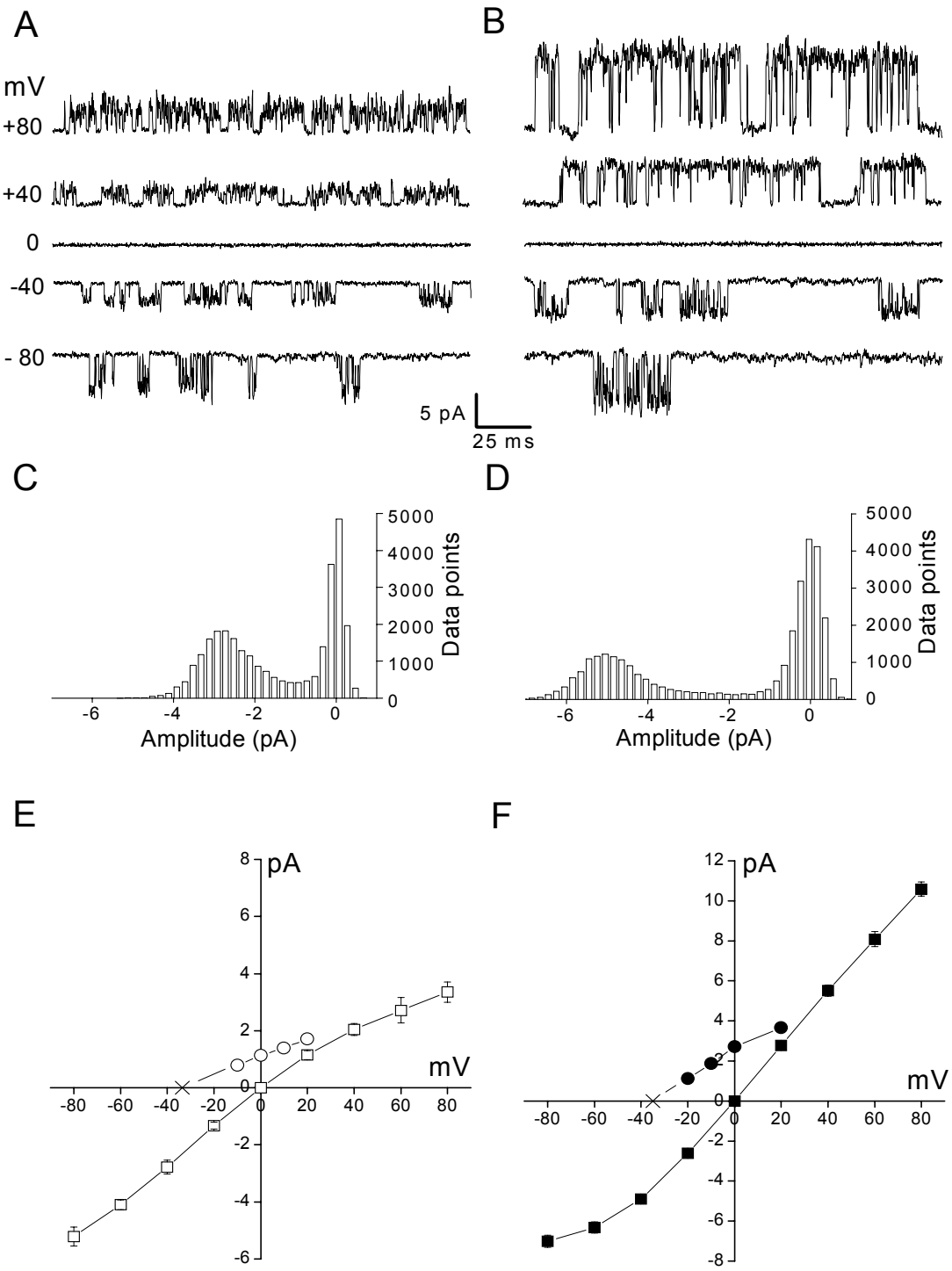

Figure 11. TREK-like channels in outside-out patches from rat cardiomyocytes
A, small conductance, inwardly rectifying channel. The transmembrane potential is indicated on the left. B, large-conductance, outwardly rectifying channel. C and D, the all-point amplitude histogram of the two channels shown in panels A and B, respectively, at -40 mV. E, single-channel currentvoltage relation of the small-conductance channel with 140 mmol/L (□) and 32 mmol/L (○) external K^+. F, single-channel current-voltage relation of the large-conductance channel with 140 mmol/L (■) and 32 mmol/L (●) external K^+. The crosses (×) indicate the extrapolated reversal potentials. Error bars were omitted when they were smaller than the size of the symbols.

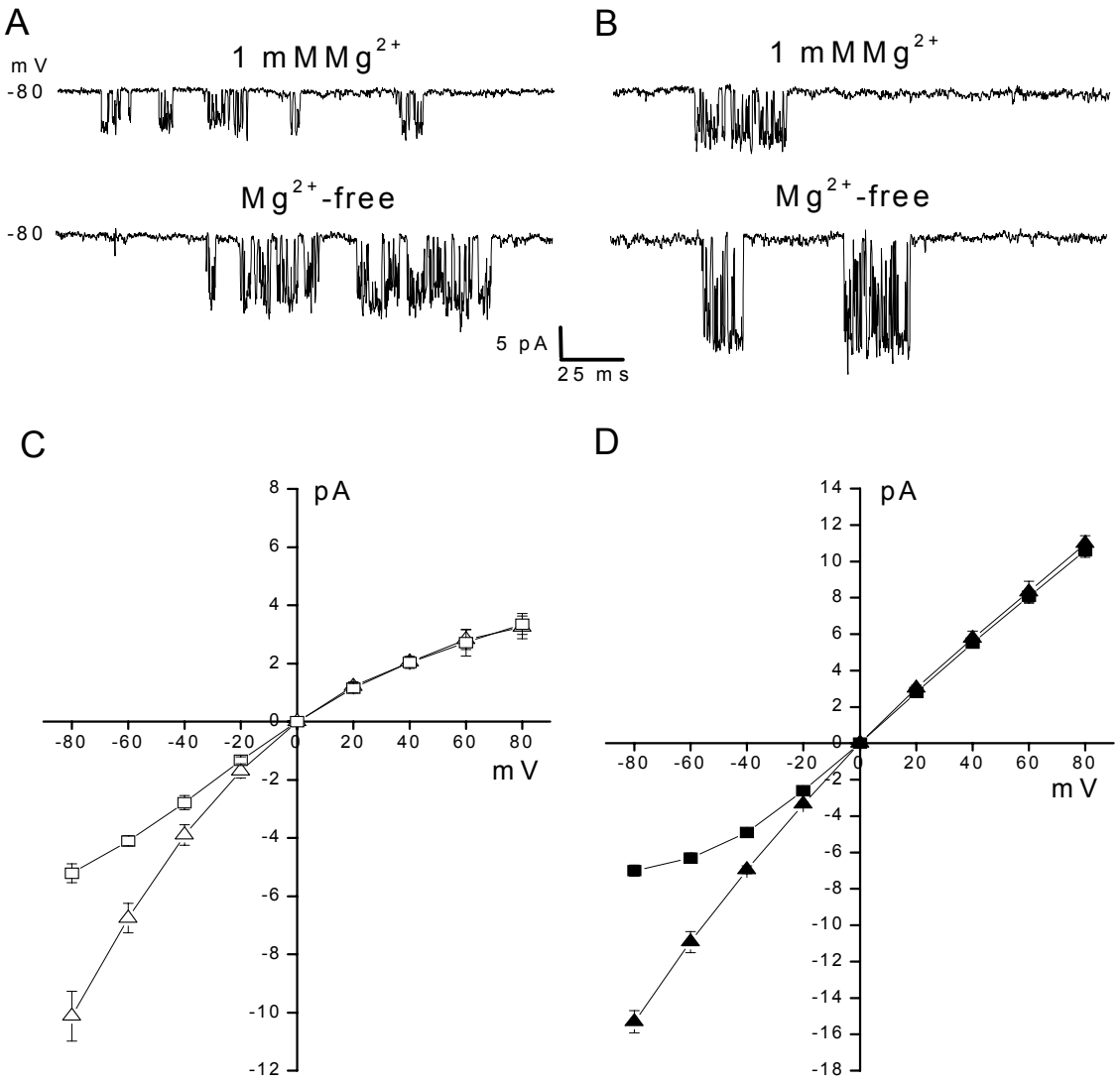

Figure 12. The conductance of both TREK-like channels depended on the presence of extracellular Mg^{2+} and single channel recording of TASK-1

A and B, typical outside-out recordings of the small-conductance (A) and the large-conductance TREK-like channel (B) in the presence or absence of 1 mM Mg^{2+} (in Ca^{2+} free, symmetrical high-K^+ solution). C, in the presence of 1 mM extracellular Mg^{2+} the slope conductance at -60 mV (g-60) of the small-conductance channel was 52.5±4.5 pS (open squares; n=4); in the absence of Mg^{2+}, g-60 was 156±15 pS (open triangles; n=5). D, in the presence of 1 mM extracellular Mg^{2+}, g-60 of the large-conductance channel was 60.7±6.0 pS (filled squares; n=10); in the absence of Mg^{2+}, g-60 was 209±12 pS (filled triangles; n=3).

divalent cations. Removal of external Mg^{2+} induced a large increase of the conductance in the inward direction. In the small-conductance channel removal of external Mg^{2+}

increased the slope conductance at -60 mV from 61±6 (n=10) to 156±15 pS (n=4; Fig. 12A and C). In the large-conductance channel removal of external Mg^{2+} increased

Figure 13. Outside-out recording of TASK-1 in rat ventricular myocytes.

the slope conductance at -60 mV from 53±5 pS (n=5) to 209±12 pS (n=3; Fig. 12B and D). We also can record the TASK-1 with single channel conductance 16.8 pS (n=5; Fig. 13) as reported previously (Kim et al., 1999) in rat cardiomyocytes.

In another series of experiments we tested the effects of various K^+ channel blockers on the smaller TREK-like channel. The current amplitude measured at +40 mV in outside-out patches was unchanged by application of 1 mM TEA (2.10±0.29 vs. 2.07±0.34 pA; n=4), 1 mM 4-aminopyridine (2.03±0.30 vs. 2.02±0.33 pA; n=3) or 1 mM $BaCl_2$ (1.97±0.36 vs. 1.94±0.31 pA; n=3). The value of NP_o measured at +40 mV was also not affected by the three drugs.

5. Regulation of the novel TREK-like channel by pH, stretch and arachidonic acid

The open probability (P_o) of the novel cardiac TREK-like K^+ channel increased with intracellular acidification (Fig. 14). Compared to control (pH 7.3), NP_o (number of channels in the patch × P_o) increased by a factor of 5.7 at pH 6.8 (n=3) and by a factor of 136 at pH 6.3 (n=3). In Fig. 16, the pH-dependent changes in NP_o are shown on a logarithmic scale (n=3). NP_o of the small-conductance TREK-like channel could be increased by changes in hydrostatic pressure applied to the patch pipette. In inside-out patches application of negative pressure (-40 cm H_2O; Fig. 15) increased NP_o by factor

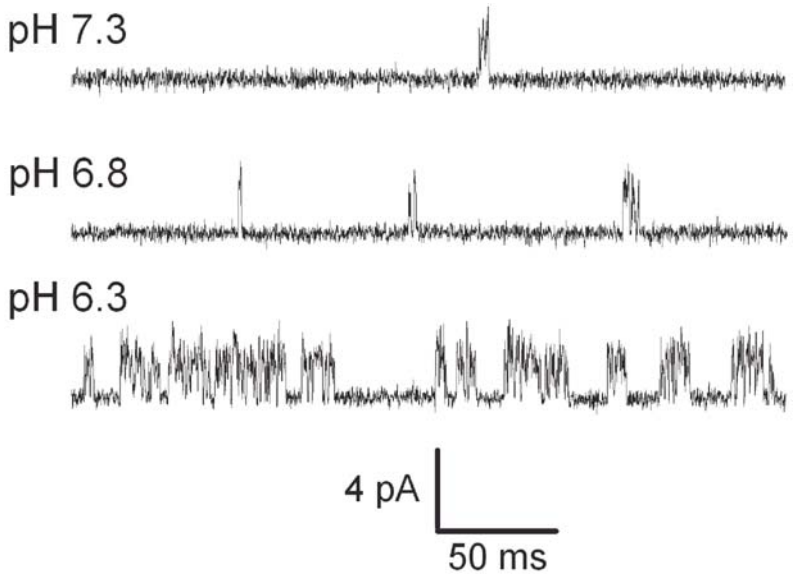

Figure 14. pH sensitivity of TREK-1 in rat ventricular myocytes
Inside-out recording at a holding potential of +40 mV at pH values of 7.3, 6.8 and 6.3.

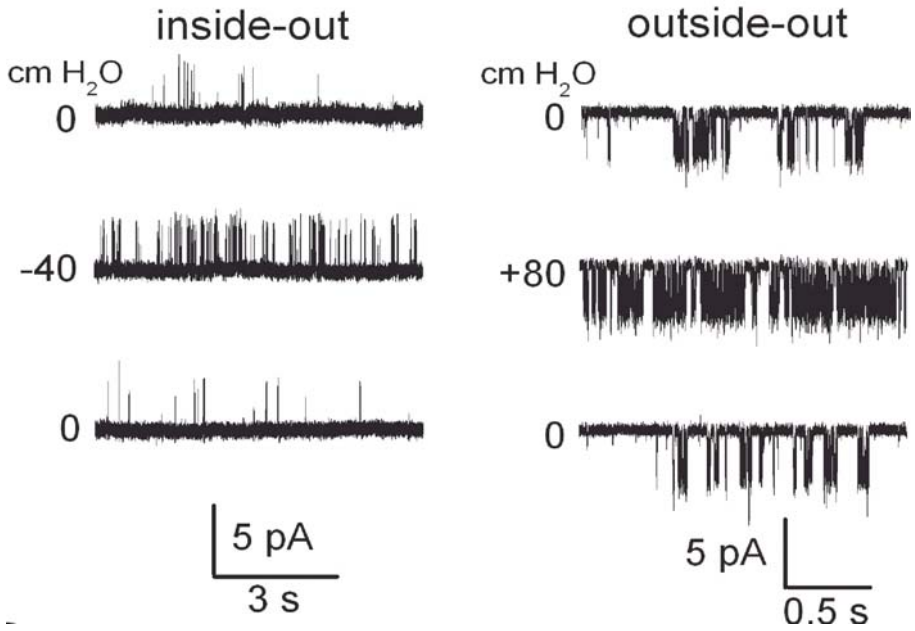

Figure 15. Stretch sensitivity of TREK-1 in rat ventricular myocytes
Left, inside-out recording before, during and after application of negative pressure (-40 cm H_2O; holding potential, +40 mV). Right, outside-out recording before, during and after application of positive pressure (+80 cm H_2O; holding potential, -40 mV). The hydrostatic pressure in the patch pipette was changed by adjusting the water level in a calibrated U-shaped glass tube using a syringe.

of ≈27, whereas application of negative pressure had no effect. In outside-out patches, positive pressure (+80 cm H_2O; Fig. 15) increased NP_o by a factor of ≈3, whereas negative pressure had no effect. Thus, in both inside-out and outside-out patches, distention of the cell membrane appeared to increase P_o. The mean values of NP_o obtained in at least three experiments are shown on a logarithmic scale in Fig. 16. Application of arachidonic acid activated the novel TREK-like channel in inside-out patches (Fig. 16). On average, NP_o increased by a factor of ≈18 during application of 10 µM arachidonic acid (n=4; Fig. 16). Thus, the novel channel shared many of the characteristic properties of the 'classical' TREK-1 channels described previously (Kim, 2003).

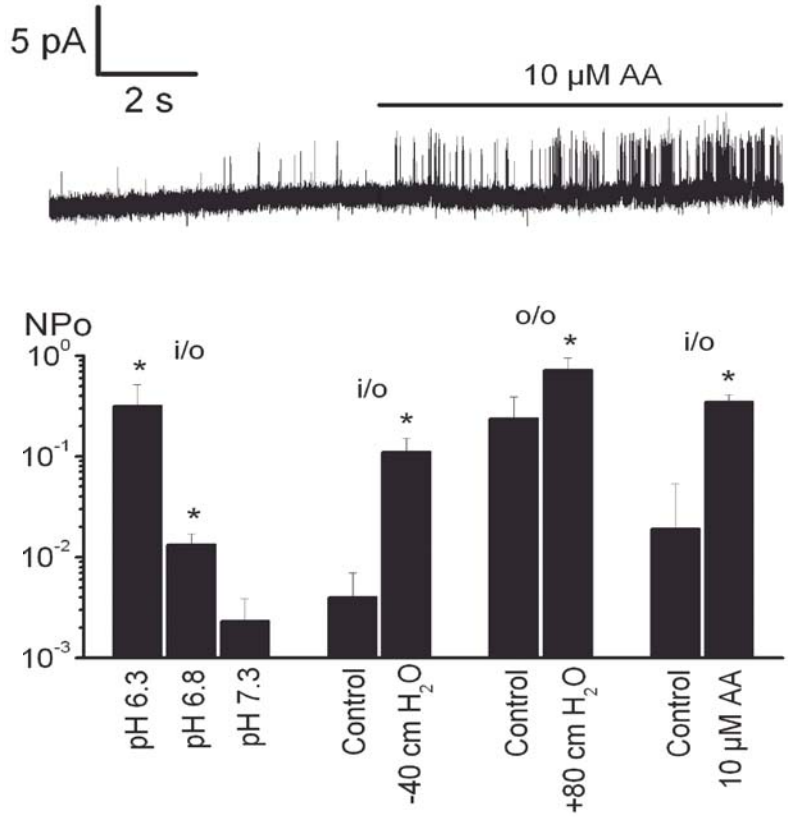

Figure 16. Response of TREK-1 to Arachidonic acid and statistic analysis
Upper, increase in NP_o produced by application of 10µM arachidonic acid in an inside-out patch at +40 mV. Bottom, statistics of the effects of intracellular acidification (inside-out), negative pressure (inside-out), positive pressure (outside-out), and arachidonic acid (inside-out) on NP_o of the small-conductance TREK-like channels, shown on a logarithmic scale. Only steady-state changes in channel activity (after >5s) were evaluated. Asterisks indicate that the changes were statistically significant (Student's t-test; $p<0.05$).

6. Heterologous expression of TREK-1a and TREK-1b channels

To test whether one of the native cardiac TREK-like K^+ channels might correspond to TREK-1 we expressed both TREK-1a and TREK-1b channels in HEK293 cells. The biophysical properties of the two splice variants were virtually identical. Surprisingly, transfection of either splice variant in HEK293 cells produced two populations of channels with different characteristics (Fig. 17). In some of the inside-out patches of TREK-1a channels (n=7) we found both a high-conductance channel reminiscent of classical TREK-1 and a low-conductance channel similar to that observed in cardiomyocytes. In the majority of inside-out patches of TREK-1a (n=11) we found only the low-conductance channel. It had a conductance of 65.8±4.6 pS (n=12) at negative potentials and 37.4±5.9 pS at positive potentials (Fig. 18); the corresponding values for TREK-1b (n=7) were 65.9±4.9 pS and 38.0±4.1 pS (Fig. 18), which is not significantly different ($p>0.05$).

The high-conductance channel in inside-out patches displayed a conductance of 105.4±24.4 pS for TREK-1a (n=4) and 96.6±27.8 pS for TREK-1b (n=3) at positive potentials. In a few cases, the nature of the channel changed from high- to low-conductance or vice versa. Fig. 17A shows an example in which a TREK-1a channel first displayed a high conductance (110 pS, upper trace), converted to a low conductance (40 pS, middle trace) two minutes later, and changed back to its earlier characteristics after another minute. In cell-attached patches, both channel types were also regularly observed, as illustrated in Fig. 17B. The simplest interpretation of these experiments is that the TREK-1 channels can assume two different functional states or ‘modes’ with different conductances.

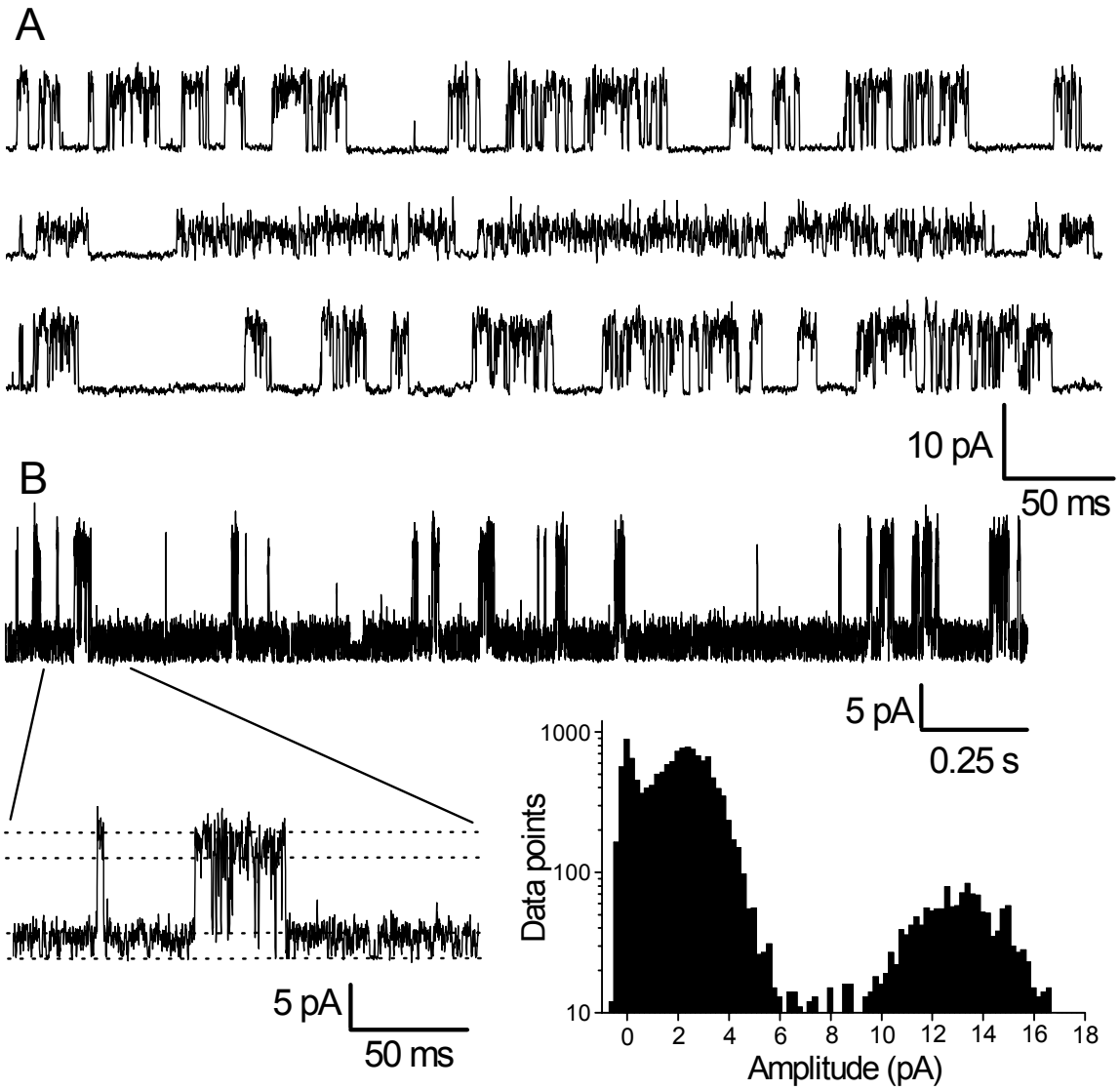

Figure 17. Two conductance modes of TREK-1 channels
A, inside-out recording at +80 mV of TREK-1a expressed in a HEK293 cell. The three traces are part of a continuous measurement; they were recorded 1 min (upper trace), 3 min (middle trace) and 4 min (lower trace) after establishment of the inside-out configuration. B, cell-attached recording from a HEK293 cell transfected with TREK-1a, taken at +80 mV with high-K^+ solution in bath and pipette. The patch contained both a high-conductance and a low-conductance channel. The all-point amplitude histogram shows a distinct peak for the opening of the low-conductance channel. The other two peaks, corresponding to the high-conductance channel alone and to the superposition of both channels are not clearly separated, due to the rapid flicker of both channels.

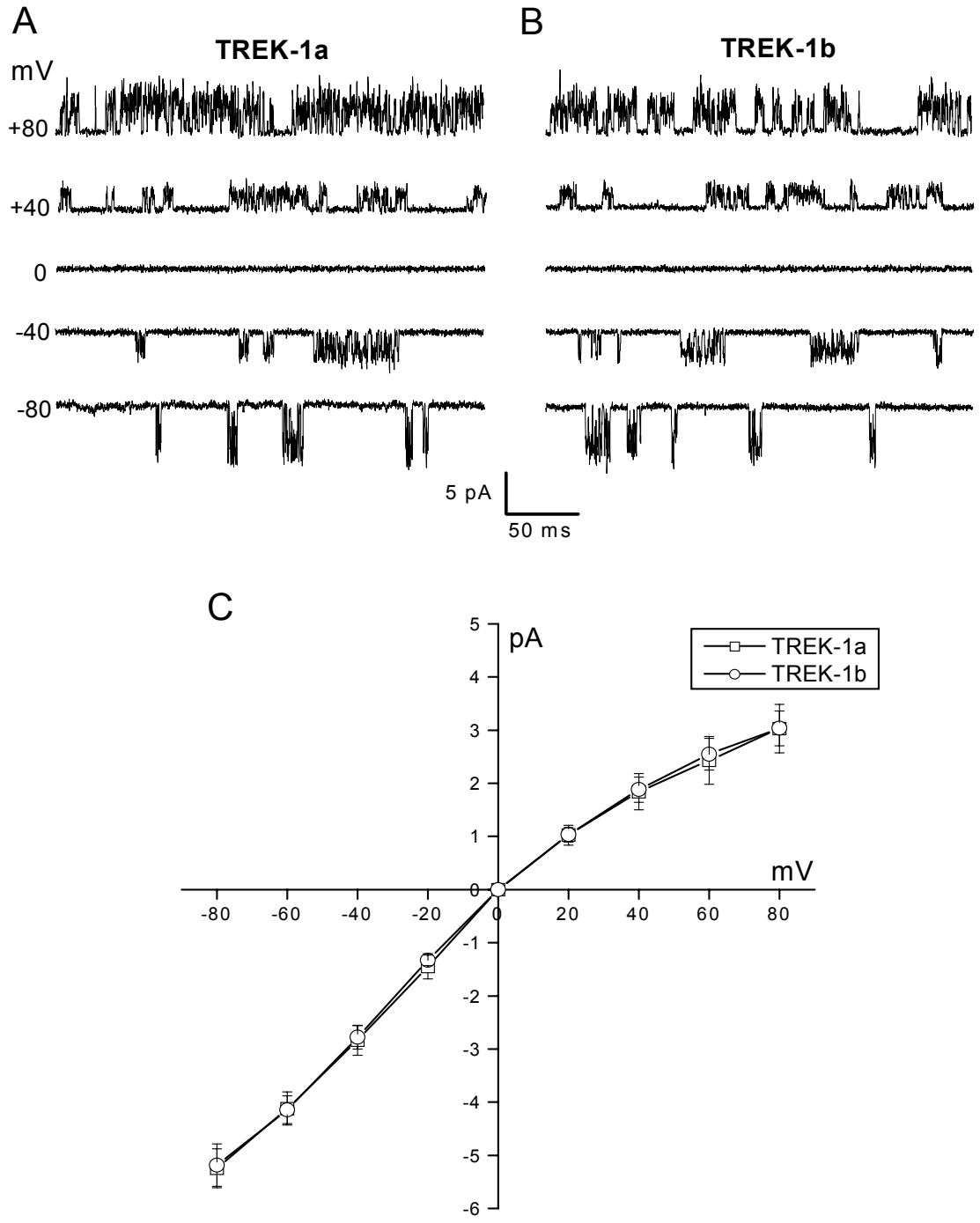

Figure 18. Comparison of TREK-1a and TREK-1b in HEK290 cell line
A, inside-out recording of TREK-1a at different membrane potential. B, inside-out recording of TREK-1b at different membrane potential. C, current-voltage relationship of TREK-1a and TREK-1b.

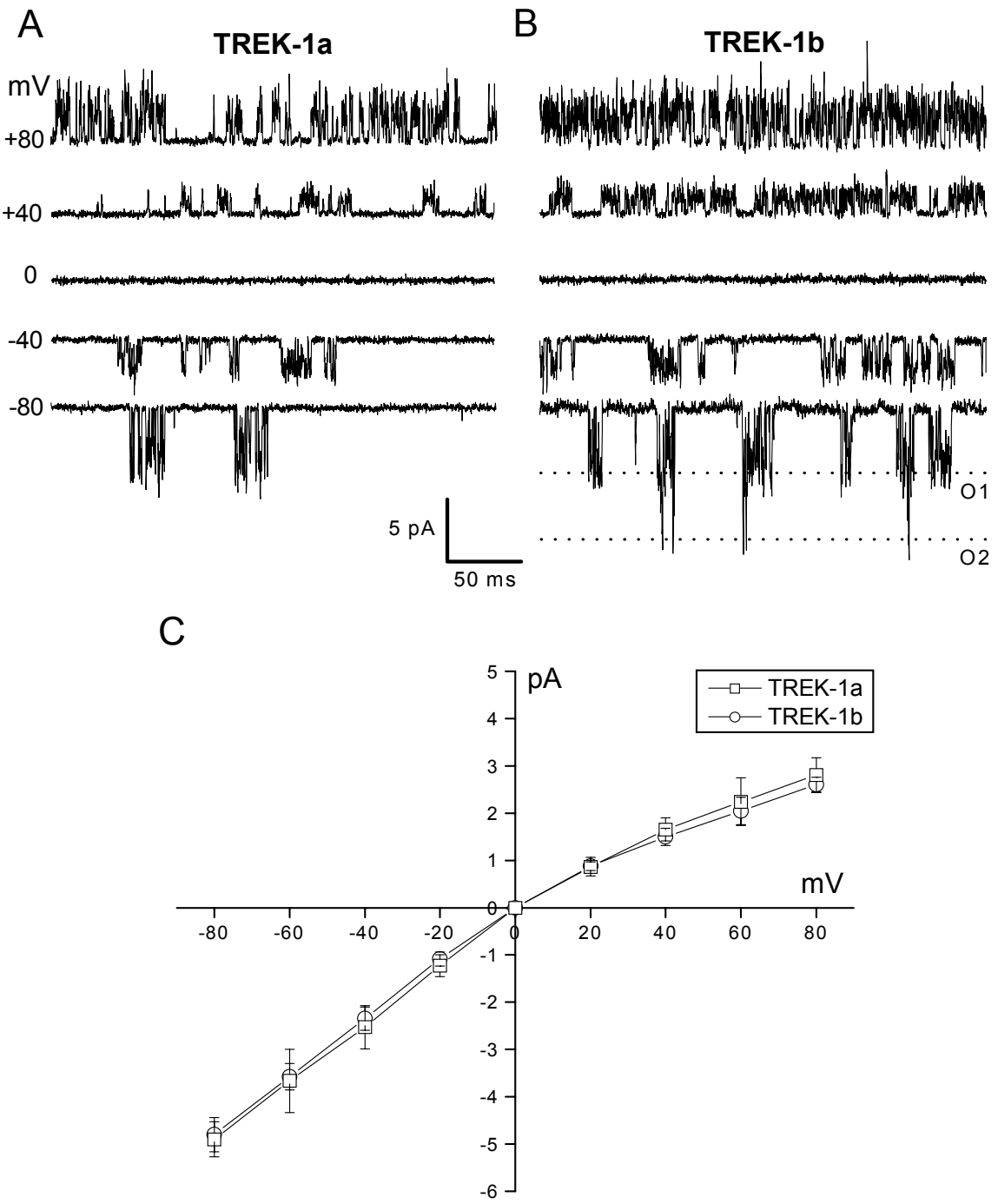

Figure 19. Comparison of TREK-1a and TREK-1b in COS-7 cell line
A, cell-attached recording of TREK-1a at different membrane potential. B, cell-attached recording of TREK-1b at different membrane potential. C, current-voltage relationship of TREK-1a and TREK-1b.

Expression of the two TREK-1 splice variants in COS-7 cells gave similar results as in HEK293 cells. Typical cell-attached measurements in COS-7 cells are shown in Figure 19. In the low-conductance mode, the mean conductance of TREK-1a was 61.2±6.4 pS at negative potentials and 34.9±5.3 pS at positive potentials (n=4); the corresponding values for TREK-1b were 60.5± 4.4 pS and 31.8±2.6 pS (n=4), which is not significantly different ($p>0.05$). In conclusion, in all patch-clamp configurations examined, two different modes of TREK-1a or TREK-1b channels were observed, but the majority of patches showed only the low-conductance mode.

7. Comparison of the cloned TREK-1 channel with native cardiac channels

Since TREK-1b is strongly expressed in rat cardiomyocytes we compared the biophysical properties of this splice variant with those of the low-conductance cardiac TREK-like channel. Fig. 20 shows typical inside-out recordings of the smaller cardiac TREK-like channel described above (panel A) and of TREK-1b channels expressed in HEK293 cells (panel B). It can be seen that the single-channel current-voltage relations (Fig. 20C, □ and △) were indistinguishable. The conductance of the cardiac channel was 67.2±1.9 pS (n=4) at negative potentials and the conductance of TREK-1b was 65.9±4.9 pS (n=7). Furthermore, the kinetics of channel opening was also very similar. Both the native and the cloned channel opened in bursts interrupted by very short closures. At +40 mV, the smaller TREK-like channel in cardiomyocytes had mean open time of 0.29±0.03 ms (n=3) and TREK-1b expressed in HEK293 cells had a mean open time of 0.28±0.03 ms (n=3). TREK-1b, like the cardiac TREK-like channels, could be activated by stretch and by intracellular acidification (not illustrated).

Fig. 20D illustrates that, despite the inward rectification of the single-channel current voltage relation, the whole-cell current in HEK293 cells transfected with

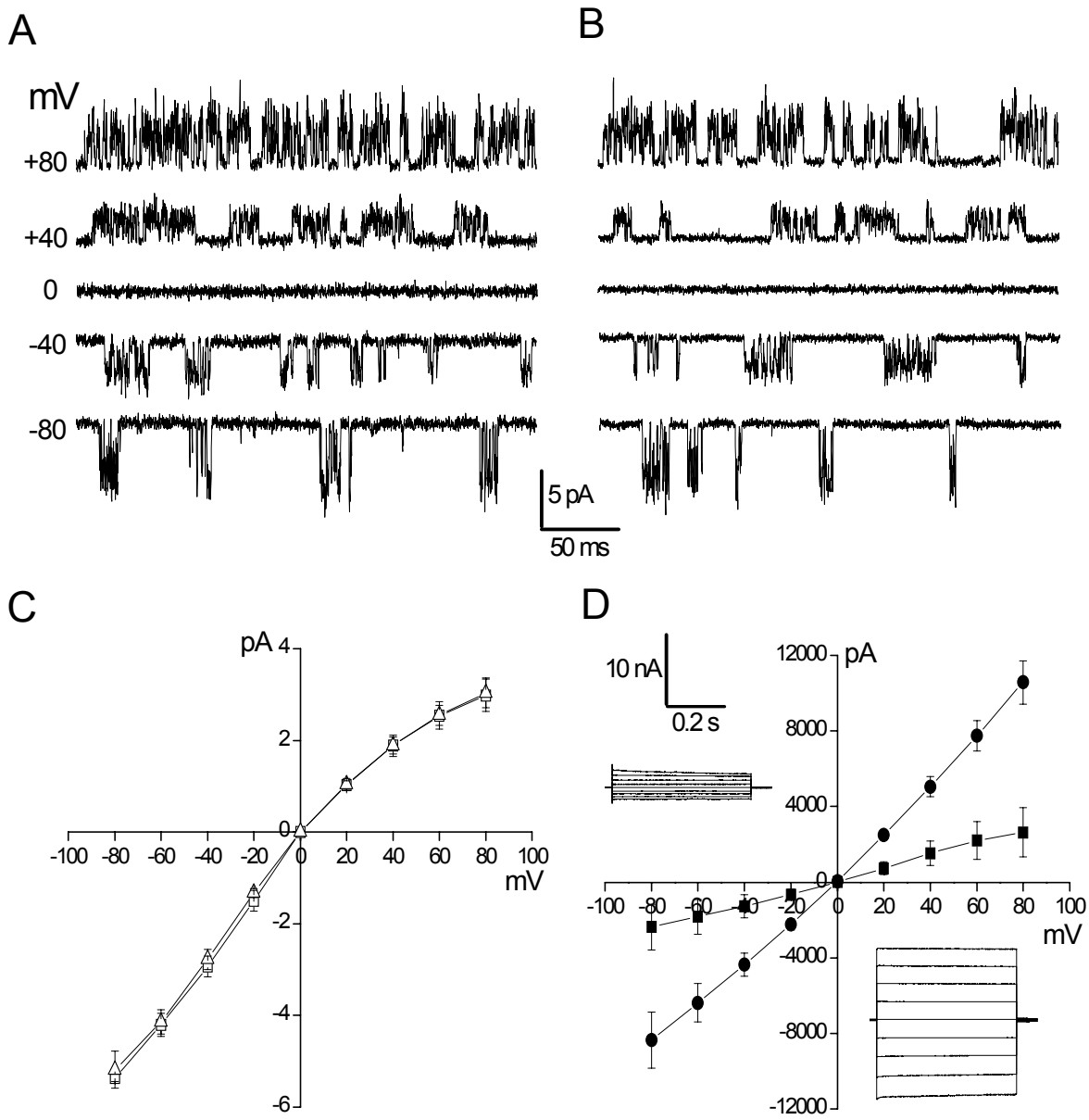

Figure 20. Comparison of cardiac TREK-like channels with cloned TREK-1b channels

A, inside-out recording of the low-conductance channel in rat cardiomyocytes. B, inside-out recording of TREK-1b expressed in HEK cells. The recordings were performed in symmetrical high-K^+ solution. Note that the gaps between bursts are shorter at positive potentials. C, inside-out current-voltage relations of transfected TREK-1b channels in HEK293 cells (△) and of the low-conductance TREK-like channel in cardiomyocytes (□). D, whole-cell current-voltage relation of HEK293 cells transfected with TREK-1b (●; n = 6) and in mock-transfected cells (■; n = 18), recorded in high-K solution. The insets show current traces obtained from transfected (lower right quadrant) and mock-transfected cells (upper left).

TREK-1b showed slight outward rectification (●). This apparent discrepancy was probably due to an increase in open probability with depolarization (Bockenhauer et al., 2001; Maingret et al., 2002), as can also be seen in Fig. 20B. Typical amplitude

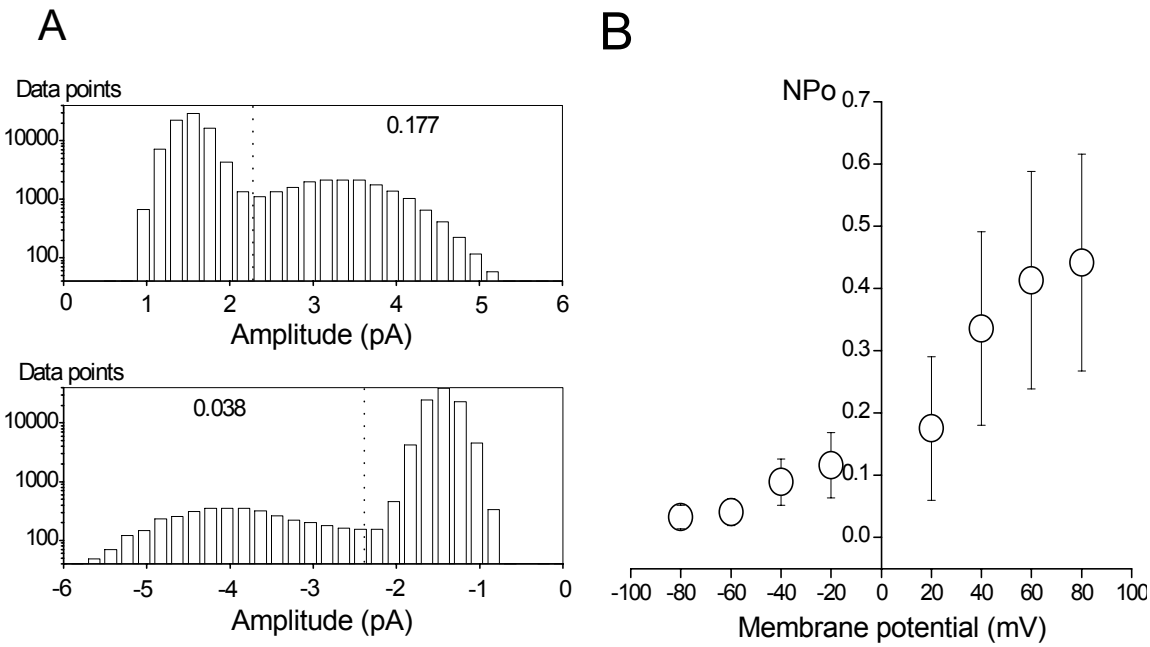

Figure 21. Open probability changes with membrane potential
A, all-point amplitude histograms measured at +40 mV (upper panel) and at -40 mV (lower panel) in an inside-out patch from a transfected HEK293 cell. The ratio of the number of data points on either side of the dotted line was calculated to obtain an estimate of NP_o. B, dependence of NP_o of TREK-1b channels on membrane potential.

histograms of a single TREK-1b channel at -40 and +40 mV is shown in Fig. 21A. NP_o was estimated by dividing the amplitude histogram at the minimum between the two peaks (dotted line) and calculating the ratio of data points corresponding to open and closed state, respectively. Fig. 21B shows that NP_o strongly increased with depolarization in the voltage range -80 to +80 mV.

The kinetics of TREK-1b channel opening were analyzed in inside-out patches from transfected HEK293 cells (Fig. 22). The membrane potential was -40 mV (left column) and +40 mV (right column), respectively. The open-time histograms (panels A and B) show a single exponential component, and the mean open times (τ_o) measured at -40 mV (0.38±0.02 ms; n=3) and at +40 mV (0.28±0.03 ms; n=3) were similar. The closed-time histogram could be fitted with two exponentials. The shorter component

(τ_{c1}, panels C and D) corresponds to the rapid closures during the burst, whereas the longer component (τ_{c2}, panels E and F) represents the gaps between bursts. τ_{c1} was similar at -40 mV (0.43±0.07 ms; n=3; panel C) and +40 mV (0.50±0.05 ms; n=3; panel D). In contrast, τ_{c2} was markedly prolonged at -40 mV (193±65 ms; n=4; panel E) as compared to +40 mV (49±34 ms; n=4; panel F). The difference was statistically significant ($p<0.01$; paired Student's t-test). The mean ratio of τ_{c2} at -40 mV to τ_{c2} at +40 mV in the same patch was 5.0±2.4. These results suggest that the lower open probability of TREK-1b channels at more negative potentials is mainly attributable to a prolongation of the gaps between bursts. The longer gaps between bursts are also apparent in the original recordings (see Fig. 20A and B).

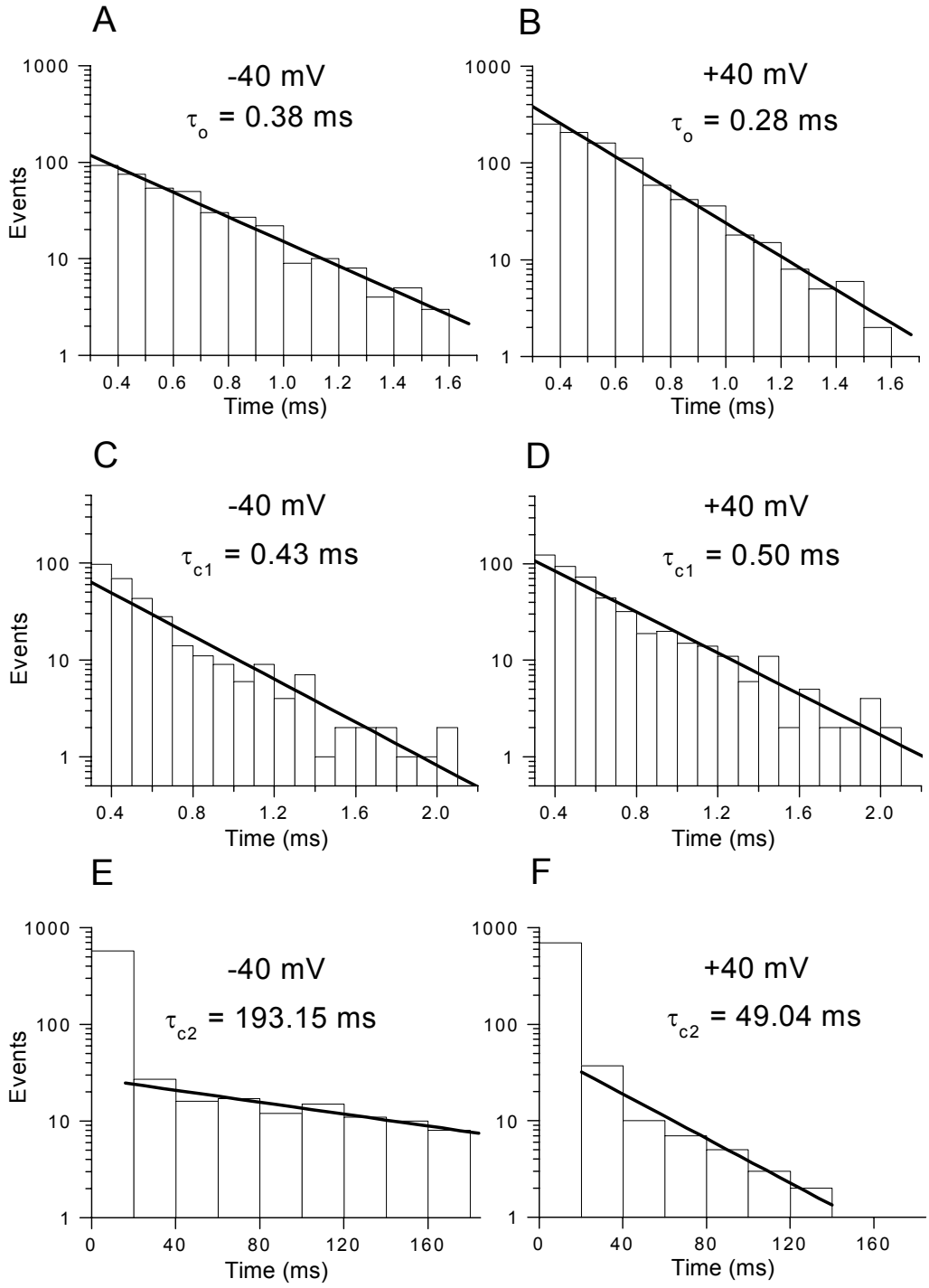

Figure 22. The kinetics of TREK-1b channel opening patches
Time histograms derived from inside-out recordings from transfected HEK293 cells in symmetrical high-K^+ solution; the membrane potential was -40 mV (left column) and +40 (right column), respectively. A and B, open-time histograms. C and D, closed-time histograms for short closures (τc1, closures during bursts). E and F, closed-time histogram for longer closures (τc2, gaps between bursts). Note that the slow component of the mean closed time, τc2, was markedly increased at -40 mV.

8. Block of TREK-1b channels by bupivacaine

The local anesthetic bupivacaine, which has been shown to block mouse and human TREK-1a channels (Kindler et al., 1990; Punke et al., 2003), may be a useful tool for clarifying the function of TREK-1 in cardiac muscle. Therefore we studied the effects of bupivacaine on rat TREK-1b channels expressed in HEK293 cells. Figure 23 illustrates that the TREK-1b whole-cell current in HEK293 cells superfused with physiological salt solution the whole-cell current carried by TREK-1b channels showed outward rectification and could be blocked by application of 1 mM bupivacaine. The control current was 10.2±2.8 nA at +80 mV and was reduced to 1.2±0.4 nA (n=6, $p<0.05$).

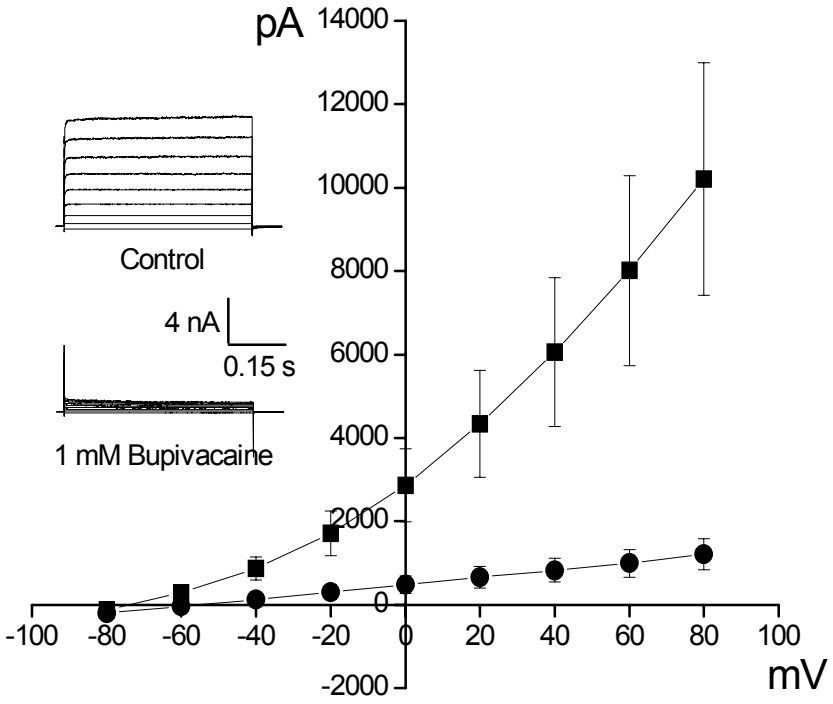

Figure 23. Effects of bupivacaine on rat TREK-1b channels expressed in HEK293 cells

Whole-cell current voltage relation of TREK-1b measured under control conditions (■; n = 6) and in the presence of 1 mM bupivacaine (●; n = 6). The insets show typical current traces.

9. Block of TREK-1b channels by forskolin

In addition to its sensitivity to arachidonic acid, TREK-1 is inhibited by cAMP via PKA phosphorylation of Ser333 in the C-terminal part of the channel structure (Patel et al., 1998). The native cardiac channel generating IK_{AA} can also be regulated by cAMP. In cell-attached experiments, CPT-cAMP, the permeant analog of cAMP, produced a complete inhibition of IK_{AA} when the current had been activated by either AA or stretch (Terrenoire et al., 2001)

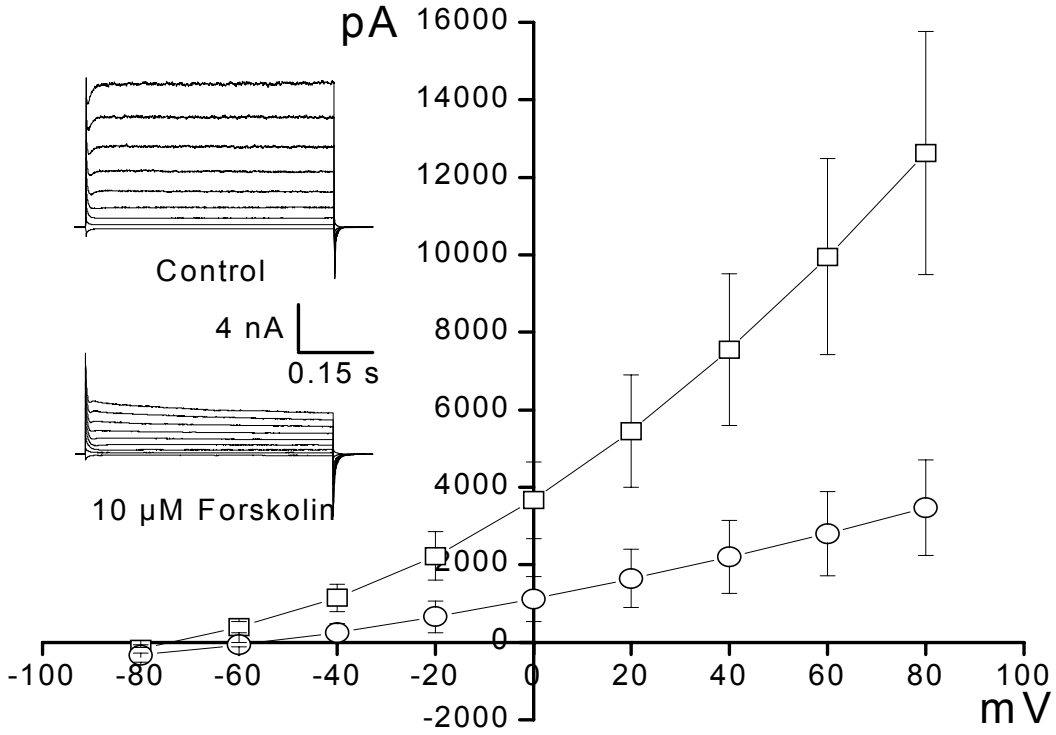

Figure 24. Effects of forskolin on rat TREK-1b channels expressed in HEK293 cells

Whole-cell current voltage relation of TREK-1b measured under control conditions (□; n = 8) and in the presence of 10 µM forskolin (O; n = 8). The insets show typical current traces.

We tested the effects of PKA phosphorylation induced by forskolin on TREK-1b (Fig. 24). Application of 10 μM forskolin produced a significant decrease from 12.6±3.1 nA to 3.5±1.2 nA at +80 mV ($n=8$, $p<0.05$).

Taken together, our single-channel measurements suggest that the two TREK-like channels found in cardiomyocytes correspond to the low- and high-conductance modes of either TREK-1 splice variant. Since TREK-1a was barely detectable in the cell-specific RT-PCR experiments, most of the cardiac channels were probably encoded by TREK-1b. Our kinetic measurements suggest that under physiological conditions the whole-cell current flowing through TREK-1 channels should be outwardly rectifying, despite the fact that, with symmetrical K^+ concentrations, the single-channel current voltage relation of the low-conductance mode showed inward rectification (Fig. 20C). The outward rectification is due, firstly, to the voltage dependence of NP_o, and, secondly, to the asymmetric K^+ concentrations across the sarcolemma.

Discussion

So far many characteristics and the functional role of cardiac background potassium TREK-1 are unknown. We employed cell-specific RT-PCR to detect the level of TREK-1 mRNA in rat ventricular muscle. Expression of two different splice variants, TREK-1a and TREK-1b, was found and re-amplification of the PCR-products suggested that TREK-1b mRNA was predominant. The localization pattern of plasma membrane TREK-1 from immunofluorescence is longitudinal stripes at the external surface and this may correspond to its function. The outwardly rectifying macroscopic K^+ selective currents were induced by mechanical stretch in rat cardomyocytes and similar currents were found after application of 10 μM arachidonic acid. Under symmetrical K^+ conditions, we observed a large TREK-1 channel with single channel conductance of 132±5 pS at positive potentials and a novel small TREK-1 channel with single channel conductance of 41±5 pS at positive potentials. The open probability of novel channel could be enhanced by intracellular acidification, arachidonic acid and stretch. Augmentation of the novel channel activity not only was induced by negative pressure at inside-out patch but also by positive pressure at outside-out patch. Apparently the way that the novel channel was activated by stretch was decided by the configuration of the patch. In heterologous expression systems (HEK293 cells and COS-7 cells), we found no significant differences between TREK-1a and TREK-1b and both show the high and the low conductance mode. Properties of TREK-1 in HEK293 or COS-7 cells are also identical to those in rat cardiomyocytes. Those results suggest there are two operative modes of TREK-1 and the low conductance mode of TREK-1 is the major one. The TREK-1 channel is the best candidate that corresponds to the stretch activated whole cell K^+ currents (I_{SAK}) since other TREK superfamily members such as TREK-2 and TRAAK were not detected in rat cardiomyocytes. It can be reasonably speculated that I_{SAK} is the opposite side of I_{SAC} that can be simultaneously activated by stretch.

1. TREK-1 channels in rat ventricular cells

1.1 Expression of TREK-1 in rat ventricular cells

RT-PCR to detect the TREK-1 (access number: U73488) was run by Tan et al and indicated TREK-1 expressed in both adult rat atrial and ventricular cells (Tan *et al.* 2002). Aimond et al. also employ the primer for TREK-1 (access number: U73488) and suggest high presence of TREK-1 in rat ventricular myocytes (Aimond *et al.* 2000). The group of Lazdunski also showed expression of TREK-1 in rat atrial (Terrenoire et al., 2001) cells. Our study carried out cell-specific RT-PCR of rat cardiomyocytes (rCMC) and employed three different primer pairs, recognizing all TREK-1 splice variants (TREK-1), TREK-1a and TREK-1b (giving two bands), or TREK-1b only, and detected robust expression of TREK-1b. Re-amplification showed very weak expression of TREK-1a as well. Previous research did not differentiate the expression level of TREK-1a and TREK-1b in cardiomyocytes by employing the cell-specific RT-PCR and different primer pairs. The first detection of rat TREK-1a and TREK-1b in cardiomyocytes is attributable to the different design of the primers.

1.2 Localization of TREK-1 in rat ventricular cells

The early work of localization of TREK-1 shows the TREK-1 staining in rat atrial cells by peroxidase-DAB method (Terrenoire et al., 2001). In the present study, immunohistochemistry with antibodies against TREK-1 showed a striking localization pattern at the plasma membrane. The wide field image of TREK-1 proteins focussed on the surface of a rat cardiomyocyte, revealed distinct longitudinal stripes. In contrast, immunostaining of TASK-1, focussed on the centre of the cell, showed transverse stripes related to the T-tubules, as has been reported previously (Jones et al., 2002). Confocal imaging showed that TREK-1 channel proteins are arranged in longitudinal stripes at the surface of cardiomyocytes. This localization pattern appears to be suitable for sensing longitudinal stretch of the cells.

2. TREK-like channels in cardiomyocytes

The first TREK-like K^+ channels in rat ventricular myocytes were recorded by Donghee Kim (Kim & Clapham., 1989; Kim & Duff., 1990; Kim., 1992). In his initial paper (Kim & Clapham., 1989) Kim found two types of potassium selective channels activated by intracellular arachidonic acid or phosphatidylcholine in neonatal rat atrial cells. In inside-out patches, arachidonic acid activated a large-conductance (160 pS, $I_{K.AA}$) outwardly rectifying potassium selective channel. Although K_{2P} channels were not known at the time, the channel described by Kim resembles large conductance TREK-1 found in our study in many respects: activation by arachidonic acid, stretch and intracellular acidification, as well as the typical 'flickery burst' kinetics. With symmetrical K^+ concentrations, the channel displayed outward rectification with a slope conductance of 106 pS at +60 mV (Kim., 1992). But 10 μM phosphatidylcholine can activate a second K^+ channel ($I_{K.PC}$) when applied to the intracellular surface of patch in initial paper (Kim & Clapham., 1989). The single channel conductance was 68 pS in the outward direction and 44 pS in the inward direction but arachidonic acid and its metabolites had no effect on channel activation. The small-conductance outward rectifier channel described by Kim differs substantially from the small conductance channel presented in our study that is inwardly rectifying and the activity of channel can be enhanced by arachidonic acid. Strangely, Kim did not mention the small conductance K^+ channel in later study.

Using rat ventricular myocytes, Kim found perfusion of the cytoplasmic side of the membrane with unsaturated fatty acid such as 10 μM arachidonic acid almost completely inhibited ATP-sensitive K^+ channels (K_{ATP}) but activated a ATP-insensitive K^+ channel with a outwardly rectifying property. When the both pipette and bath solutions contain 140 mM K^+, the single channel conductance was 150 pS in outward current direction and 82 pS in inward current direction (Kim & Duff., 1990). In 1992, Kim described a mechanosensitive potassium channel in adult rat atrial cells with a slope conductance of 94±11 pS at +60 mV and 64±8 pS at –60 mV with symmetrical high K^+ conditions. Mechanical stimulation, arachidonic acid and intracellular acidosis also can activate the channel.

The group of Lazdunski used negative pressure and arachidonic acid stimulation in inside-out patch confirmed presence of $I_{K.AA}$ in adult Wistar rat atrial cells. The corresponding current-voltage curves were outwardly rectifying both in physiological and in symmetrical K^+ conditions, with chord conductances at +50 mV of 41±1 pS and 118±4 pS, respectively (Terrenoire et al., 2001). A similar ventricular stretch-activated pH sensitive channel was later found by Tan et al (2002). In adult rat ventricular myocytes at symmetrical 150mM K^+, this channel displayed a nearly linear current-voltage relation with a slope conductance of 111±3 pS at positive potential. The channel was not blocked by 4-AP, TEA and glibenclamide.

The high-conductance TREK-like channel described in the present study showed outward rectification and had a conductance of 132 pS at positive potentials. Thus, its properties were in reasonable agreement with the channels observed previously in rat ventricular (Kim & Duff., 1990; Tan et al., 2002) and atrial muscle (Kim., 1992; Shui & Boyett., 2000; Terrenoire et al., 2001). Similar to the native channels, the high-conductance channels observed after transfection of rat TREK-1a and TREK-1b in HEK293 cells showed outward rectification in symmetrical high-K^+ solution and had a mean conductance of about 100 pS at positive potentials. These findings are consistent with the data reported previously for mouse TREK-1a (95-130 pS) (Patel et al., 1998; Koh et al., 2001; Honore et al., 2002; Han et al., 2003; Kang et al., 2005). Rat TREK-1b expressed in *Xenopus* oocytes was found to have a conductance of 85 pS with 100 mM K^+ solution (Bockenhauer et al., 2001), which may translate to ~100 pS with 150 mM K^+.

The low-conductance cardiac K^+ channel described in this thesis is clearly different: it showed inward rectification with a mean conductance of 66 pS at negative and 41 pS at positive potentials. It was found in ~60 % of outside-out patches, about four times more frequently than the high-conductance TREK-like channel. The following considerations suggest that this novel channel was also encoded by TREK-1: (i) its single-channel current-voltage relation was indistinguishable from that of the low-conductance mode TREK-1a or TREK-1b expressed in HEK cells; (ii) its kinetics were very similar to those of the low-conductance mode of TREK-1b; (iii) both channels were activated by stretch and intracellular acidification; (iv) TREK-1b was

robustly expressed in cardiomyocytes, whereas the two other stretch-sensitive K^+ channels, TREK-2 and TRAAK, could not be detected. Since TREK-1a was barely detectable by cell-specific RT-PCR, most of the cardiac low- and high-conductance TREK-like channels were probably encoded by TREK-1b.

After carefully checking the previous articles, we did not find other reports of the small inwardly rectifying K^+ channel in heart tissue before. But the Kim group recently found four different arachidonic-acid-activated TREK-like K^+ channels in magnocellular hypothalamic neurons (Han et al., 2003). One of these channels (denoted $i_{K.AA3}$), which was observed more frequently than the others, had properties almost identical to the low-conductance cardiac channel described here. A search run by Kim group in GenBank for a DNA sequence similar to those of TREK-1, TREK-2 or TRAAK failed to yield any novel TREK-like K^+ channel gene.

3. Properties of TREK-like potassium channel

3.1 Stretch activation of TREK-1

NP_o of the small-conductance TREK-like channel could be increased by changes in hydrostatic pressure applied to the patch pipette. In inside-out patches application of negative pressure (-40 cm H_2O; Fig. 15 in Results) increased NP_o but application of negative pressure had no effect. In outside-out patches, positive pressure (+80 cm H_2O; Fig. 15 in Results part) increased NP_o but application of negative pressure had no effect. Thus, in both inside-out and outside-out patches, distension of the cell membrane appeared to increase P_o. So far people only found that negative pressure can activate TREK-1 like potassium channels with both cell-attached and inside-out configuration (Kim., 1992; Patel et al., 1999; Lesage et al., 2000). We reported for the first time that positive pressure activates the channels in the outside-out configuration. So it is worth speculating on the mechanism in order to understand the channel better. After suction, the membrane patch of cell-attached and inside-out can be formed and the piece membrane is concave. When applying negative pressure by pipette, the curvature of membrane becomes larger and consequently the channel activity is enhanced. In outside-out configuration, the original membrane shape is convex. Application of positive pressure by pipette pushes the patch membrane and

makes the membrane more convex and resulted in stimulating the channel (Fig. 25). In either case we have distension (stretch) of the membrane and increase in curvature.

Analysis of deletion and chimeric mutants indicated that activation of TREK-2 by fatty acid and membrane stretch involves a distinct molecular mechanism (Kim et al., 2001). Protonation of E306 drastically tightens channel–phospholipid interaction and leads to TREK-1 opening at atmospheric pressure (Chemin J et al., 2004). But there is very poor knowledge of the mechanism that stretch activates the TREK-1 channel.

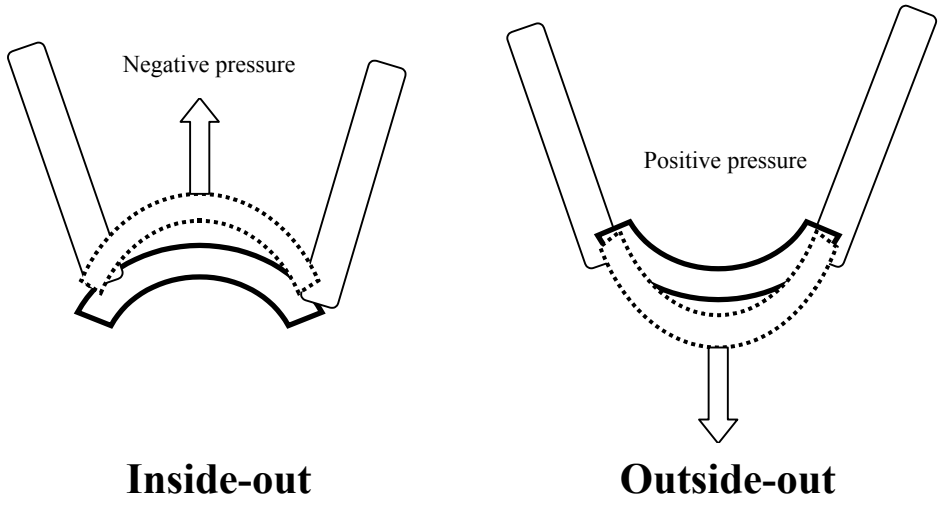

Figure 25. Schematic of different direction pressure works on different patch configuration
Left, in inside-out or cell-attached mode, suction deforms patch membrane from control (solid line) to stretch shape (dashed line). The arrow shows the direction of pressure. Right, in outside-out mode, positive pressure changes the patch membrane from control (solid line) to stretch shape (dashed line), The arrow shows the direction of pressure.

3.2 Voltage-dependent activity of TREK-1

Despite the inward rectification of the single-channel current voltage relation, the whole-cell current in HEK293 cells transfected with TREK-1b showed slight outward rectification. This apparent discrepancy was probably due to an increase in open probability with depolarization (Bockenhauer et al., 2001; Maingret et al., 2002). Fig. 21 (in Results part) shows that NP_o strongly increased with depolarization in the voltage range -80 to +80 mV. Kinetic analysis suggests that the lower open probability

of TREK-1b channels at more negative potentials is mainly attributable to a prolongation of the gaps between bursts. Deletional and chimeric analysis demonstrates that the carboxy terminal domain of TREK-1 is responsible for voltage-dependent gating (Maingret et al., 2002). We speculate that outward rectification of TREK-1 in rat cardiomyocytes would favour channel opening at depolarized potentials and contribute to the shortening of the action potential

Other K_2P channel such as TASK-3 also displays similar properties. Cell-attached patch-clamp recordings of TASK-3 expressed in HEK293 cells showed that the single channel current-voltage relation was inwardly rectifying and open probability increased markedly with depolarization. The outward rectification found in the whole-cell currents may be reconciled with the inward rectification of the single K^+ channels by taking into account the marked increase in open probability observed at positive potentials (Rajan et al., 2000).

3.3 Divalent cations regulate the single channel conductance

The conductance of both TREK-like channels depended on the presence of extracellular divalent cations. Removal of external Mg^{2+} induced a large increase of the conductance in the inward direction. In the small-conductance channel removal of external Mg^{2+} increased the slope conductance at -60 mV from 61±6 to 156±15 pS. In the large-conductance channel removal of external Mg^{2+} increased the slope conductance at -60 mV from 53±5 pS to 209±12 pS. The group of Lazdunski also found mouse TREK-1 activity, in transiently transfected COS cells, is reduced at negative resting membrane potentials by external Mg^{2+} (Maingret et al., 2002).

Our group's previous works also suggested when divalent cations were omitted from the pipette solution, the mean single channel (outward) current of TASK-3 at +100 mV was nearly unchanged, whereas the inward current at +100 mV was about twice as large as in the presence of external divalent cations. E70 is an important determinant of sensitivity of extracellular divalent cations in TASK-3 and mutation of this glutamate to lysine (E70K) led to reduced the channel sensitivity to above ions (Derst et al., 2002). It is unknown to which residue response to Mg^{2+} block of TREK-1 and it will be answered in future.

3.4 Two operating modes of TREK-1

Transfection of either TREK-1 splice variant in HEK293 cells produced two populations of channels with different characteristics (Fig. 17 in Results). In some of the inside-out patches of TREK-1a channels we found both a high-conductance channel reminiscent of classical TREK-1 and a low-conductance channel similar to that observed in cardiomyocytes. In the majority of inside-out patches of TREK-1a we found only the low-conductance channel.

Comparison of TREK-1a and TREK-1b channels in HEK293 and COS-7 cells showed that their properties were virtually identical. Both splice variants displayed a low- and a high-conductance mode, and both modes were regulated by physical and chemical stimuli in a very similar way. Apparently the low- and high-conductance modes of splice variants do not represent the subconductances because in this case sublevels should only be observed in the presence of main state activity (Fox, 1987). The simplest explanation for our surprising observation of two channel modes is that covalent modification of the channel or interaction with an accessory intracellular protein may induce a second conformational state of TREK-1 channels with a different conductance. Variation in the nature or extent of glycosylation may provide a mechanism. It is also possible that the two conductance modes are related to mechanical tension of the membrane or to interaction of the channel protein with phospholipids (Chemin et al., 2005). A recent study suggested that sumoylation kept the plasma membrane TWIK-1 channel silent (Rajan et al., 2005) and we can speculate that sumoylation may play a role in two operative modes of TREK-1.

In guinea-pig cardiomyocytes, it was reported that there was a novel K^+ channel that represented a different 'mode' of the classical inward rectifier channel in which opening occurs only at very negative potentials. In cell-attached recordings the novel channel frequently converted to a classical inward rectifier channel, and *vice versa*. This conversion was not voltage dependent. After excision of the patch, the novel channel always converted to a classical inward rectifier channel within 0–3 min. This conversion was not affected by intracellular Mg^{2+}, phosphatidylinositol (4,5)-bisphosphate or spermine (Liu et al., 2002).

The biophysical characteristics of two modes of TREK-1 channel activity described here are quite different from the two open states of TREK-1 channels observed by Bockenhauer *et al.* In the presence of Mg^{2+}, which were "consistent with unblocked and blocked current levels at negative potentials" (Bockenhauer et al., 2001). Our findings are in line with the results of Han et al (2003) who found four different arachidonic-acid-activated TREK-like K^+ channels in magnocellular hypothalamic neurons. One of these channels (denoted $i_{K.AA3}$), which was observed more frequently than the others, had properties almost identical to the low-conductance cardiac channel described here, whereas the other endogenous K^+ channels showed the properties of 'classical' high-conductance TREK-1, TREK-2 and TRAAK.

3.5 Block by bupivacaine

Punke et al found that bupivacaine inhibited human TREK-1 channels in a concentration-dependent and reversible manner (Punke et al., 2003). Bupivacaine also blocked the other K_2P member TASK-3 (Kim et al., 2000). Our study also suggested that bupivacaine strongly inhibited TREK-1 current in HEK293 cells. Bupivacaine like lidocaine and is a local anaesthetic. The modulation function of bupivacaine on K_2P channels may link to work mechanism of local anaesthetic. Local anaesthetic such as lidocaine and bupivacaine may block K_2P background K^+ currents and depolarised the membrane potential, consequently, reduced the excitation of cells (depolarisation block). This effect may contribute the effects of local anaesthetic.

3.6 Regulation by phosphorylation

TREK-1 is inhibited by cAMP via PKA phosphorylation of Ser333 in the C-terminal part of the channel structure (Patel et al., 1998). The native cardiac channel generating IK_{AA} can also be regulated by cAMP. In cell-attached experiments, CPT-cAMP, the permeant analog of cAMP, produced a complete inhibition of IK_{AA} when the current had been activated by either AA or stretch (Terrenoire et al., 2001). Our study indicated that PKA induced by forskolin blocked TREK-1b in HEK293 cells. Such a TREK-1 channel might contribute to the positive inotropic effects produced by β-adrenergic stimulation of the heart. It is well known that the upregulation of the β-

adrenergic activity produces the positive inotropic effects by activation of voltage-dependent Ca^{2+} channels and the simultaneous inhibition of TREK-1 could contribute to the positive inotropic effect by inducing a prolongation of the action potential and thus a further increase in Ca^{2+} influx.

TREK-1 is not only inhibited by PKA-dependent phosphorylation through Gαs-coupled receptors but also inhibited by PKC-dependent phosphorylation by Gαq-coupled receptors (Murbartian et al., 2005). There are two TREK-1 phosphorylation sites that are required for PKA-, PKC- and receptor-mediated inhibition: a previously described PKA site at Ser-333 and a novel site at Ser-300. Progressive dephosphorylation at whole cell configuration contributes to the TREK-1 current 'run-up' that currents increase with time (Murbartian et al., 2005).

Other K_2P channel members also regulated by G protein coupling receptor. In hypoglossal motoneurones and cerebellar granule cells, these TASK-like currents are inhibited by different neurotransmitters known to stimulate Gq/11-coupled receptors (acetylcholine, serotonin, norepinephrine, thyrotropin- releasing hormone, substance P, and glutamate). Co-expressing a Gq coupled receptor and the cloned TASK channel in transfected cells also produced similar results (Millar et al., 2000; Talley et al., 2000).

3.7 Activation by arachidonic acid

One of the basic characteristics of TREK-1 is that AA can activate it. There is the natural asymmetric distribution of the negatively charged phosphatidylserines in the inner leaflet of the plasma membrane and some lipids (as for instance arachidonic acid) tend to preferentially insert in the external leaflet of the bilayer, leading to a convex curvature of the membrane. The change of membrane curvature might lead to the opening of TREK-1 (Sheetz et al., 1974). An alternative hypothesis is that compounds with a smaller polar head and a large hydrophobic tail, such as AA, are considered as cones with the base of the cone at its hydrophobic tail and the membrane is deformed by insertion of cone (AA)-shaped lipids. Then the deformation of membrane makes the TREK-1 open (Patel et al., 2001).

4. Stretch-activated whole-cell currents in cardiac muscle

Confocal imaging showed that TREK-1 channel proteins are arranged in longitudinal stripes at the surface of cardiomyocytes. This localization pattern appears to be suitable for sensing longitudinal stretch of the cells. In cells superfused with physiological salt solution, stretch activated a large outward current at positive potentials that was probably attributable to activation of both SACs and SAKs (Kamkin et al., 2000; Isenberg et al., 2003). We succeeded in isolating the current component flowing through SAKs by applying only moderate stretch, by selecting cells that showed only little current through SACs and by inhibiting other current components with a blocker cocktail. The remaining stretch-activated whole-cell current showed outward rectification and was probably carried by both the 'classical' high-conductance (Kim., 1992; Terrenoire et al., 2001; Niu & Sachs., 2003) and the novel low-conductance TREK-like channels. It should be noted, however, that we studied only steady-state current changes. Single-channel recordings of stretch-activated TREK-like K^+ channels in rat atrium (Niu & Sachs., 2003) showed substantial inactivation (or adaptation) with a time constant of ≈1 s. Thus, the phasic stretch-activated K^+ current flowing during myocardial stretch *in vivo*, for example at the end of diastole during high preload, may be much larger than the steady-state outward current shown here. Furthermore, TREK-1 currents are expected to be much larger at 37 °C (Kang et al., 2005).

5. The possible functional role of TREK-1 channels in the heart

5.1 Cardiac protection in ischemia or hypoxia

The cardiac TREK-1 channel may play an important role in protecting against cell damage caused by ischemia, which is known to elevate intracellular levels of certain fatty acids, including arachidonic acid (Schror et al., 1987)

During ischemia or hypoxia, the intracellular pH decreases and may consequently activate the TREK-1 in cardiomyocytes. Opening of TREK-1 can induce hyperpolarization of membrane potential and close the voltage-gated Ca^{2+} channel, which lead to influx of Ca^{2+}, further protecting the cells from ischemic or hypoxia

damage. Recently, the role of TREK-1 in polyunsaturated fatty acid and lysophospholipids-induced neuroprotection was further indicated by the genetic inactivation of TREK-1. TREK-1(–/–) mice display an increased sensitivity to both ischaemia and epilepsy; Activation of TREK-1 by volatile anesthetics can protect the neuron(Heurteaux et al., 2004). A recent study suggests that TREK-1 and its activation by arachidonic acid is resistant to hypoxia (Buckler et al., 2005). So those results suggest the TREK-1 not only tolerates hypoxia but also antagonizes the damage of hypoxia to protect the tissue.

In glomus cells, hypoxia inhibited a TASK-1 potassium channel, which was characterized by weak voltage dependence, low activity upon extracellular acidosis and a unitary conductance recorded in cell attached patches of 14 pS (Buckler et al., 2000). A 14-pS K^+ channel with kinetic properties similar to those of TASK-1 was identified in rat atrial and ventricular cells (Kim et al., 1999). So interesting question is raised whether the inhibition of TASK-1 mediated by hypoxia is counterbalance to activation of TREK-1 by hypoxia in cardiomyocytes. But first we must get evidence that hypoxia really enhances the TREK-1 activity in heart.

5.2 Counterbalance of SACs

In the beating heart, stretch may activate both SACs and SAKs. The net effect of stretch applied during diastole is usually a depolarization that may initiate ventricular premature beats or even fibrillation when it reaches threshold (Franz et al., 1992; Zabel et al., 1996; Zeng et al., 2000; Janse et al., 2003; Ravens., 2003). However, arrhythmogenesis may not be the only function of SACs and SAKs; it is conceivable that they may also play a role in the length-dependent regulation of contractile force of cardiomyocytes.

Rapid stretch of cardiac muscle produces an instantaneous change in isometric force of contraction, which is followed by slow increase in force over several minutes. This slow force response (SFR, also denoted the Anrep effect) is associated with a slow increase in the magnitude of the intracellular calcium transient (Allen & Kentish., 1985; Nichols et al., 1988). It has been proposed that opening of I_{SAC} contributes to the slow length dependent changes in the force of contraction (Lab et al., 1994; Tavi et al.,

1998; Calaghan & White., 2004). At diastolic negative potentials SACs are predominantly carried by Na^+ ions (Isenberg et al., 2003), i.e. stretch of the myocytes during the ventricular filling phase is thought to increase the submembrane Na^+ concentration, which in turn augments the cellular Ca^{2+} load via Na^+-Ca^{2+} exchange (NCX) (Tavi et al., 1998; Perez et al., 2001). The resulting increased filling of the intracellular Ca^{2+} stores (Lab et al., 1994; Tavi et al., 1998; Perez et al., 2001; Calaghan & White., 2004) might contribute to the slow force response observed after an increase in preload.

Previous reports showed that neither L-type Ca^{2+} currents (Hongo et al., 1996) nor the sarcoplasmic reticulum (SR) (Kentish et al., 1998) contribute to the increase in Ca^{2+} transient during the SFR. Other reports suggested that stretch triggered an autocrine/paracrine mechanism that activated the Na^+-H^+ exchange (NHE), increased the $[Na^+]i$ and subsequently Ca^{2+} entry through the reverse mode of Na^+-Ca^{2+} exchange (Perez et al., 2001).

These considerations suggest that Na^+ influx through SACs or NHE during the late filling phase of the cardiac cycle may make a major contribution to the slow force response (Lab et al., 1994; Tavi et al., 1998; Calaghan & White., 2004; Cingolani et al., 1998), and the same mechanisms may also be responsible for arrhythmogenic afterpotentials (Tavi et al., 1998). The simultaneous opening of SAKs might serve to prevent excessive diastolic depolarization under conditions of high preload. Thus, one of the major functions of TREK-like channels in cardiomyocytes may be to counterbalance the inward current produced by activation of I_{SAC} and to prevent the occurrence of ventricular extrasystoles.

Summary

Cardiac TREK-1 like potassium channels play an important role in the function of cardiomyocytes. A novel low-conductance TREK-1 like potassium channel and a high-conductance TREK-1 like potassium channel in rat cardiomyocytes are described in this thesis. The biophysical properties of the two cardiac TREK-like channels were similar to those of TREK-1a or TREK-1b channels expressed in HEK293 cells, which both displayed a low- and a high-conductance mode.

- Using cell-specific RT-PCR we found strong expression of a splice variant of rat TREK-1, denoted TREK-1b, in which the N-terminus is extended by 15 amino acids compared to the 'classical' TREK-1a channel protein.
- Immunohistochemistry with antibodies against TREK-1 showed localization of the channel in longitudinal stripes at the external surface membrane of cardiomyocytes.
- When the cardiomyocytes were mechanically stretched using a glass stylus, an outwardly rectifying K^+ current component could be detected in whole-cell recordings.
- In single-channel recordings with symmetrical high K^+ solution, two TREK-like channels with 'flickery-burst' kinetics were found: a ‘high-conductance’ K^+ channel (132±5 pS at positive potentials) and a novel ‘low-conductance’ channel (41±5 pS at positive potentials). The low-conductance channel could be activated by negative pressure in inside-out, positive pressure in outside-out patches, intracellular acidification and arachidonic acid. Its open probability was strongly increased by depolarization, due to decreased duration of gaps between bursts.
- The biophysical properties of the two cardiac TREK-like channels were similar to those of TREK-1a or TREK-1b channels expressed in HEK293 cells, which both displayed a low- and a high-conductance mode. Our results suggest that the

TREK-like channels found in rat cardiomyocytes may reflect two different modes of TREK-1.

- The current flowing through these mechano-gated channels may serve to counterbalance the inward current flowing through stretch-activated non-selective cation channels during the filling phase of the cardiac cycle and thus to prevent the occurrence of ventricular extrasystoles.

References

Aimond F, Rauzier JM, Bony C, Vassort G (2000). Simultaneous activation of p38 MAPK and p42/44 MAPK by ATP stimulates the K^+ current ITREK in cardiomyocytes. J Biol Chem 275, 39110-39116.

Allen DG, Kentish JC (1985). The cellular basis of the length-tension relation in cardiac muscle. J Mol Cell Cardiol 17, 821-840.

Bai X, Bugg GJ, Greenwood SL, Glazier JD, Sibley CP, Baker PN, Taggart MJ, Fyfe GK (2005). Expression of TASK and TREK, two-pore domain K^+ channels, in human myometrium. Reproduction 129(4), 525-30.

Bockenhauer D, Zilberberg N, Goldstein SA (2001). KCNK2: reversible conversion of a hippocampal potassium leak into a voltage-dependent channel. Nat Neurosci 4, 486-491.

Buckler KJ, Williams BA, Honore E (2000). An oxygen-, acid- and anaesthetic-sensitive TASK-like background potassium channel in rat arterial chemoreceptor cells. TASK channels are implicated in the peripheral chemoreceptor response to reduced oxygen tension. J Physiol 525, 135–142.

Buckler KJ, Honore E (2005). The lipid-activated two-pore domain K^+ channel TREK-1 is resistant to hypoxia: implication for ischaemic neuroprotection. J Physiol 562, 213-222.

Campanucci VA, Brown ST, Hudasek K, O'kelly IM, Nurse CA, Fearon IM (2005). O(2) sensing by recombinant twik-related halothane-inhibitable K(+) channel-1 background K(+) channels heterologously expressed in human embryonic kidney cells. Neuroscience, Epub ahead of print.

Calaghan S, White E (2004). Activation of Na^+-H^+ exchange and stretch-activated channels underlies the slow inotropic response to stretch in myocytes and muscle from the rat heart. J Physiol 559, 205-214.

Chavez RA, Gray AT, Zhao BB, Kindler CH, Mazurek MJ, Mehta Y, Forsayeth JR, Yost CS (1999). TWIK-2, a new weak inward rectifying member of the tandem pore domain potassium channel family. J Biol Chem 274, 7887-7892.

Chemin J, Patel AJ, Duprat F, Lauritzen I, Lazdunski M, Honore E (2005). A phospholipid sensor controls mechanogating of the K^+ channel TREK-1. Embo J 24, 44-53.

Cingolani HE, Alvarez BV, Ennis IL, Camilion de Hurtado MC (1998). Stretch-induced alkalinization of feline papillary muscle: an autocrine-paracrine system. Circ Res 83, 775-780.

Clarke CE, Veale EL, Green PJ, Meadows HJ, Mathie A (2004). Selective block of the human 2-P domain potassium channel, TASK-3, and the native leak potassium current, IKSO, by zinc. J Physiol 560, 51-62.

Czirjak G, Enyedi P (2002). Formation of functional heterodimers between the TASK-1 and TASK-3 two-pore domain potassium channel subunits. J Biol Chem 277, 5426–5432.

Czirjak G , Enyedi P (2002). TASK-3 dominates the background potassium conductance in rat adrenal glomerulosa cells. Mol Endocrinol 16, 621–629.

Czirjak G, Enyedi P (2003). Ruthenium red inhibits TASK-3 potassium channel by interconnecting glutamate 70 of the two subunits. Mol Pharmacol 63, 646–652.

Czirjak G, Fischer T, Spat A, Lesage F, Enyedi P (2000). TASK (TWIK-related acid-sensitive K^+ channel) is expressed in glomerulosa cells of rat adrenal cortex and inhibited by angiotensin II. Mol Endocrinol 14, 863–874.

Derst C, Liu GX, Musset B, Rajan S, Preisig-Müller R, Daut J (2002). Molecular analysis of divalent cation sensitivity of TASK channels. Pflugers Arch 443 (S2), S340, 44-10.

De Miera EVS, Lau DHP, Zhadina M, Pountney D, Coetzee WA, Rudy B (2001). KT3.2 and KT3.3, two novel human two-pore K^+ channels closely related to TASK-1. J Neurophysiol 86, 130–142.

Duprat F, Lesage F, Fink M, Reyes R, Heurteaux C, Lazdunski M (1997). TASK, a human background K^+ channel to sense external pH variations near physiological pH. Embo J 16, 5464-5471.

Duprat F, Lesage F, Patel AJ, Fink M, Romey G, Lazdunski M (2000). The neuroprotective agent riluzole activates the two P domain K^+ channels TREK-1 and TRAAK. Mol Pharmacol 57, 906-912.

Fink M, Duprat F, Lesage F, Reyes R, Romey G, Heurteaux C, Lazdunski M (1996). Cloning, functional expression and brain localization of a novel unconventional outward rectifier K^+ channel. Embo J 15, 6854-6862.

Fox JA (1987). Ion-channel subconductance states. Journal of membrane biology 97,1-8.

Franz MR, Burkhoff D, Yue DT, Sagawa K (1989). Mechanically induced action potential changes and arrhythmia in isolated and in situ canine hearts. Cardiovasc Res 23, 213-223.

Franz MR, Cima R, Wang D, Profitt D, Kurz R (1992). Electrophysiological effects of myocardial stretch and mechanical determinants of stretch-activated arrhythmias. Circulation 86, 968-978.

Girard C, Duprat F, Terrenoire C, Tinel N, Fosset M, Romey G, Lazdunski M, Lesage F (2001). Genomic and functional characteristics of novel human pancreatic 2P domain K^+ channels. Biochem Biophys Res Commun 282, 249–256.

Goldstein SAN, Wang KW, Ilan N, Pausch M (1998). Se- frequence and function of the two P domain potassium channels: implications of an emerging superfamily. J Mol Med 76, 13–20.

Gu W, Schlichthorl G, Hirsch JR, Engels H, Karschin C, Karschin A, Derst C, Steinlein OK, Daut J (2002). Expression pattern and functional characteristics of two novel splice variants of the two-pore-domain potassium channel TREK-2. J Physiol 539, 657-668.

Hamill OP, Sakmann B (1981). Multiple conductance states of single acetylcholine receptor channels in embryonic muscle cells. Nature 294, 462-464.

Han J, Gnatenco C, Sladek CD, Kim D (2003). Background and tandem-pore potassium channels in magnocellular neurosecretory cells of the rat supraoptic nucleus. J Physiol 546, 625-639.

Hartness ME, Lewis A, Searle GJ, O'Kelly I, Peers C, Kemp PJ (2001). Combined antisense and pharmacological approaches implicate hTASK as an airway O_2 sensing K^+ channel. J Biol Chem 276, 26499–26508.

Heurteaux C, Guy N, Laigle C, Blondeau N, Duprat F, Mazzuca M, Lang-Lazdunski L, Widmann C, Zanzouri M, Romey G, Lazdunski M (2004). TREK-1, a K^+ channel involved in neuroprotection and general anesthesia. Embo J 23, 2684-2695.

Hongo K, White E, Le Guennec JY, Orchard CH (1996). Changes in $[Ca^{2+}]i$, $[Na^+]i$ and Ca^{2+} current in isolated rat ventricular myocytes following an increase in cell length. J Physiol (Lond) 491, 609–619.

Honore E, Maingret F, Lazdunski M, Patel AJ (2002). An intracellular proton sensor commands lipid- and mechano-gating of the K^+ channel TREK-1. Embo J 21, 2968-2976.

Isenberg G, Kazanski V, Kondratev D, Gallitelli MF, Kiseleva I, Kamkin A (2003). Differential effects of stretch and compression on membrane currents and $[Na^+]c$ in ventricular myocytes. Prog Biophys Mol Biol 82, 43-56.

Isenberg G, Klockner U (1982). Calcium tolerant ventricular myocytes prepared by preincubation in a "KB medium". Pflugers Arch 395, 6-18.

Janse MJ, Coronel R, Wilms-Schopman FJ, de Groot JR (2003). Mechanical effects on arrhythmogenesis: from pipette to patient. Prog Biophys Mol Biol 82, 187-195.

Jones SA, Morton MJ, Hunter M, Boyett MR (2002). Expression of TASK-1, a pH-sensitive twin-pore domain K^+ channel, in rat myocytes. Am J Physiol Heart Circ Physiol 283, H181-185.

Kamkin A, Kiseleva I, Isenberg G (2000). Stretch-activated currents in ventricular myocytes: amplitude and arrhythmogenic effects increase with hypertrophy. Cardiovasc Res 48, 409-420.

Kamkin A, Kiseleva I, Wagner KD, Bohm J, Theres H, Gunther J, Scholz H (2003). Characterization of stretch-activated ion currents in isolated atrial myocytes from human hearts. Pflugers Arch 446, 339-346.

Karschin C, Wischmeyer E, Preisig-Müller R, Rajan S, Derst C, Grzeschik KH, Daut J, Karschin A (2001). Expression pattern in brain of TASK-1, TASK-3, and a tandem pore domain K^+ channel subunit, TASK-5, associated with the central auditory nervous system. Mol Cell Neurosci 18, 632–648.

Kang D, Mariash E, Kim D (2004). Functional expression of TRESK-2, a new member of the tandem-pore K^+ channel family. J Biol Chem 279, 28063-28070.

Kang D, Choe C, Kim D (2005). Thermosensitivity of the two-pore domain K^+ channels TREK-2 and TRAAK. J Physiol 564, 103-116.

Kentish JC, Wrzosek A (1998). Changes in force and cytosolic Ca^{2+} concentration after length changes in isolated rat ventricular trabeculae. J Physiol(Lond) 506, 431– 444.

Kim D (1992). A mechanosensitive K^+ channel in heart cells. Activation by arachidonic acid. J Gen Physiol 100, 1021-1040.

Kim D (2003). Fatty acid-sensitive two-pore domain K^+ channels. Trends Pharmacol Sci 24, 648-654.

Kim D, Clapham DE (1989). Potassium channels in cardiac cells activated by arachidonic acid and phospholipids. Science 244, 1174-1176.

Kim D, Duff RA (1990). Regulation of K^+ channels in cardiac myocytes by free fatty acids. Circ Res 67, 1040-1046.

Kim D, Fujita A, Horio Y, Kurachi Y (1998). Cloning and functional expression of a novel cardiac two-pore background K^+ channel (cTBAK-1). Circ Res 82 , 513–518.

Kim Y, Bang H, Kim D (1999). TBAK-1 and TASK-1, two-pore K^+ channel subunits: kinetic properties and expression in rat heart. Am J Physiol Heart Circ Physiol 277, H1669-H1678.

Kim Y, Bang H, Kim D (2000). TASK-3, a new member of the tandem pore K^+ channel family. J Biol Chem. 275, 9340–9347.

Kim Y, Bang H, Gnatenco C, Kim D (2001). Synergistic Interaction and the Role of C-Terminus in the Activation of TRAAK K^+ Channels by Pressure, Free Fatty Acids and Alkali. Pflugers Arch 442, 64-72.

Kim Y, Gnatenco C, Bang H, Kim D (2001).Localization of TREK-2 K^+ channel domains that regulate channel kinetics and sensitivity to pressure, fatty acids and pHi. Pflugers Arch 442, 952-960.

Kindler CH, Yost CS, Gray AT (1999). Local anesthetic inhibition of baseline potassium channels with two pore domains in tandem. Anesthesiology 90, 1092-1102.

Koh SD, Monaghan K, Sergeant GP, Ro S, Walker RL, Sanders KM, Horowitz B (2001). TREK-1 regulation by nitric oxide and cGMP-dependent protein kinase. An essential role in smooth muscle inhibitory neurotransmission. J Biol Chem 276, 44338-44346.

Koizumi S, Lipp P, Berridge MJ, Bootman MD (1999). Regulation of ryanodine receptor opening by lumenal Ca^{2+} underlies quantal Ca^{2+} release in PC12 cells. J Biol Chem 274, 33327-33333.

Lab MJ, Zhou BY, Spencer CI, Horner SM, Seed WA (1994). Effects of gadolinium on length-dependent force in guinea-pig papillary muscle. Exp Physiol 79, 249-255.

Leonoudakis D, Gray AT, Winegar BD, Kindler CH, Harada M, Taylor DN, Chavez RA, Forsayeth JR, Yost CS (1998). An open rectifier potassium channel with two pore domains in tandem cloned from rat cerebellum. J Neurosci 18, 868–877.

Lesage F, Guillemare E, Fink M, Duprat F, Lazdunski M, Romey G, Barhanin J (1996). TWIK-1, a ubiquitous human weakly inward rectifying K^+ channel with a novel structure. Embo J 15, 1004-1011.

Lesage F, Lauritzen I, Duprat F, Reyes R, Fink M, Heurteaux C, Lazdunski M (1997). The structure, function and distribution of the mouse TWIK-1 K^+ channel. FEBS Lett 402, 28-32.

Lesage F, Terrenoire C, Romey G, Lazdunski M (2000). Human TREK2, a 2P domain mechano-sensitive K^+ channel with multiple regulations by polyunsaturated fatty acids, lysophospholipids, and Gs, Gi, and Gq protein-coupled receptors. J Biol Chem 275, 28398-28405.

Lewis A, Hartness ME, Chapman CG, Fearon IM, Meadows HJ, Peers C, Kemp PJ (2001). Recombinant hTASK1 is an O_2- sensitive K^+ channel. Biochem Biophys Res Commun 285, 1290–1294.

Liu GX, Derst C, Schlichthorl G, Heinen S, Seebohm G, Bruggemann A, Kummer W, Veh RW, Daut J, Preisig-Muller R (2001a). Comparison of cloned Kir2 channels with native inward rectifier K^+ channels from guinea-pig cardiomyocytes. J Physiol 532, 115-126.

Liu GX, Hanley PJ, Ray J, Daut J (2001b). Long-chain acyl-coenzyme A esters and fatty acids directly link metabolism to K^+(ATP) channels in the heart. Circ Res 88, 918-924.

Liu GX, Daut J (2002). "Sleepy" inward rectifier channels in guinea-pig cardiomyocytes are activated only during strong hyperpolarization. J Physiol 539, 755-765.

Lopes CMB, Gallagher PG, Buck ME, Butler MH, Goldstein SA (2000). Proton block and voltage gating are potassium-dependent in the cardiac leak channel Kcnk3. J Biol Chem 275, 16969–16978.

Maingret F, Patel AJ, Lazdunski M, Honoré E (2001). The endocannabinoid anandamide is a direct and selective blocker of the background K^+ channel TASK-1. Embo J 20, 47–54.

Maingret F, Honore E, Lazdunski M, Patel AJ (2002). Molecular basis of the voltage-dependent gating of TREK-1, a mechano-sensitive K^+ channel. Biochem Biophys Res Commun 292, 339-346.

Meadows HJ. Randall AD (2001). Functional characterisation of human TASK-3, an acid-sensitive two-pore domain potassium channel. Neuropharmacology 40, 551–559.

Meadows HJ, Chapman CG, Duckworth DM, Kelsell RE, Murdock PR, Nasir S, Rennie G, Randall AD (2001). The neuroprotective agent sipatrigine (BW619C89) potently inhibits the human tandem pore-domain K^+ channels TREK-1 and TRAAK. Brain Res 892, 94-101.

Medhurst AD, Rennie G, Chapman CG, Meadows H, Duckworth MD, Kelsell RE, Gloger II, Pangalos MN (2001). Distribution analysis of human two pore domain potassium channels in tissues of the central nervous system and periphery. Brain Res Mol Brain Res 86,101-114.

Millar JA, Barratt L, Southan AP, Page K, Fyffe RE, Robertson B, Mathie A (2000). A functional role for the two-pore domain potassium channel TASK-1 in cerebellar granule neurons. Proc Natl Acad Sci USA 97, 3614–3648.

Murbartian J, Lei Q, Sando JJ, Bayliss DA (2005). Sequential phosphorylation mediates receptor-and kinase-induced inhibition of TREK-1 background potassium channels. J Biol Chem Jul 8, Epub ahead of print.

Nerbonne JM, Nichols CG, Schwarz TL, Escande D (2001). Genetic manipulation of cardiac K^+ channel function in mice: what have we learned, and where do we go from here? Circ Res 89, 944-956.

Nichols CG, Hanck DA, Jewell BR (1988). The Anrep effect: an intrinsic myocardial mechanism. Can J Physiol Pharmacol 66, 924-929.

Nie X, Arrighi I, Kaissling B, Pfaff I, Mann J, Barhanin J, Vallon V (2005). Expression and insights on function of potassium channel TWIK-1 in mouse kidney. Pflugers Arch, online

Niu W, Sachs F (2003). Dynamic properties of stretch-activated K^+ channels in adult rat atrial myocytes. Prog Biophys Mol Biol 82, 121-135.

O'Kelly I, Stephens RH, Peers C, Kemp PJ (1999). Potential identification of the O^{2-} sensitive K^+ current in a human neuroepithelial body-derived cell line. Am J Physiol Lung Cell Mol Physiol 276, L96–L104.

Orias M, Velazquez H, Tung F, Lee G, Desir GV (1997). Cloning and localization of a double-pore K^+ channel, KCNK1: exclusive expression in distal nephron segments. Am J Physiol 273, F663–F666.

Patel AJ, Honoré E, Lesage F, Fink M, Romey G, Lazdunski M (1999). Inhalational anaesthetics activate two-pore-domain background K^+ channels. Nat Neurosci 2, 422-426.

Patel AJ, Honore E (2003). 2P domain K^+ channels: novel pharmacological targets for volatile general anesthetics. Adv Exp Med Biol 536, 9-23.

Patel AJ, Honore E, Maingret F, Lesage F, Fink M, Duprat F, Lazdunski M (1998). A mammalian two pore domain mechano-gated S-like K^+ channel. Embo J 17, 4283-4290.

Patel AJ, Lazdunski M, Honore E (2001). Lipid and mechano-gated 2P domain K^+ channels. Curr Opin Cell Biol 13, 422-428.

Perez NG, de Hurtado MC, Cingolani HE (2001). Reverse mode of the Na^+-Ca^{2+} exchange after myocardial stretch: underlying mechanism of the slow force response. Circ Res 88, 376-382.

Preisig-Muller R, Mederos y Schnitzler M, Derst C, Daut J (1999). Separation of cardiomyocytes and coronary endothelial cells for cell-specific RT-PCR. Am J Physiol 277, H413-416.

Punke MA, Licher T, Pongs O, Friederich P (2003). Inhibition of human TREK-1 channels by bupivacaine. Anesth Analg 96, 1665-1673.

Rajan S, Plant LD, Rabin ML, Butler MH, Goldstein SA (2005). Sumoylation silences the plasma membrane leak K^+ channel K2P1. Cell 121(1), 37-47.

Rajan S, Wischmeyer E, Karschin C, Preisig-Muller R, Grzeschik KH, Daut J, Karschin A, Derst C (2000). THIK-1 and THIK-2, a novel subfamily of tandem pore domain K^+ channels. J Biol Chem 276, 7302–7311.

Rajan S, Wischmeyer E, Xin Liu G, Preisig-Muller R, Daut J, Karschin A, Derst C (2000). TASK-3, a novel tandem pore domain acid-sensitive K^+ channel. An extracellular histidine as pH sensor. J Biol Chem 275, 16650-16657.

Ravens U (2003). Mechano-electric feedback and arrhythmias. Prog Biophys Mol Biol 82, 255-266.

Reyes R, Duprat F, Lesage F, Fink M, Salinas M, Farman N, Lazdunski M (1998). Cloning and expression of a novel pH-sensitive two pore domain K^+ channel from human kidney. J Biol Chem 273, 30863-30869.

Sano Y, Inamura K, Miyake A, Mochizuki S, Kitada C, Yokoi H, Nozawa K, Okada H, Matsushime H, Furuichi K (2003). A novel two-pore domain K^+ channel, TRESK, is localized in the spinal cord. J Biol Chem 278, 27406-27412.

Schror K (1987). Eicosanoids and myocardial ischaemia. Basic Res Cardiol Suppl 1, 235-243.

Sheetz MP, Singer SJ (1974). Biological membranes as bilayer couples. A molecular mechanism of drug-erythocyte interactions**.** Proc Natl Acad Sci USA 71, 4457-4461.

Shui Z, Boyett MR (2000). A novel background potassium channel in rat atrial cells. Exp Physiol 85, 355-361.

Snyders DJ (1999). Structure and function of cardiac potassium channels. Cardiovasc Res 42, 377-390.

Taggart P (1996). Mechano-electric feedback in the human heart. Cardiovasc Res 32, 38-43.

Talley EM, Lei Q, Sirois JE, Bayliss DA (2000). TASK-1, a two-pore domain K^+ channel, is modulated by multiple neurotransmitters in motoneurons. Neuron 25, 399–410.

Talley EM, Sirois JE, Lei Q, Bayliss DA (2003). Two-pore-Domain (KCNK) potassium channels: dynamic roles in neuronal function. Neuroscientist 9, 46-56.

Talley EM, Solórzano G, Lei Q, Kim D, Bayliss DA (2001). CNS distribution of members of the two-pore-domain (KCNK) potassium channel family. J Neurosci 21, 7491–7505.

Tan JH, Liu W, Saint DA (2002). Trek-like potassium channels in rat cardiac ventricular myocytes are activated by intracellular ATP. J Membr Biol 185, 201-207.

Tan JH, Liu W, Saint DA (2004). Differential expression of the mechanosensitive potassium channel TREK-1 in epicardial and endocardial myocytes in rat ventricle. Exp Physiol 89, 237-242.

Tavi P, Han C, Weckstrom M (1998). Mechanisms of stretch-induced changes in $[Ca^{2+}]$i in rat atrial myocytes: role of increased troponin C affinity and stretch-activated ion channels. Circ Res 83, 1165-1177.

Terrenoire C, Lauritzen I, Lesage F, Romey G, Lazdunski M (2001). A TREK-1-like potassium channel in atrial cells inhibited by beta-adrenergic stimulation and activated by volatile anesthetics. Circ Res 89, 336-342.

Tucci PJ, Bregagnollo EA, Spadaro J, Cicogna AC, Ribeiro MC (1984). Length dependence of activation studied in the isovolumic blood-perfused dog heart. Circ Res 55, 59–66.

Von Anrep G (1912). On the part played by the suprarenals in the normal vascular reactions on the body. J Physiol (Lond) 45, 307–317.

Zabel M, Koller BS, Sachs F, Franz MR (1996). Stretch-induced voltage changes in the isolated beating heart: importance of the timing of stretch and implications for stretch-activated ion channels. Cardiovasc Res 32, 120-130.

Zeng T, Bett GC, Sachs F (2000). Stretch-activated whole cell currents in adult rat cardiac myocytes. Am J Physiol Heart Circ Physiol 278, H548-557.

Abbreviations

ATP	Adenosine triphosphate
bp	Base pairs
cAMP	Cyclic adenosine mono phosphate
cDNA	Complementary DNA
cRNA	Complementary RNA
DMEM	Dulbecco's modified Eagles's medium
DNA	De-oxy-ribo-nucleic acid
DNase	Deoxyribonuclease
dNTP	Deoxyribonucleotide
DTT	Dithiothreitol
E.coli	Escherichia coli
EDTA	Ethylenediaminetetraacetate
EGFP	Enhanced green fluorescent protein
HEK cells	Human embryonic kidney cells
HEPES	N-(2-hydroxyethyl)piperazineN'-2(hydroxy)propanesolphonic acid
kb	Kilo base pairs
kDa	Kilo Dalton
mM	milli molar
PCR	Polymerase chain reaction
PKA	Protein kinase A
PKC	Protein kinase C
RNA	Ribo-nucleic acid
RNase	Ribonuclease
rpm	Revolutions per minute
RT	Reverse transcription
TASK	TWIK related Acid Sensitive K^+ channel
THIK	Tandem pore domain Halothane Inhibited K^+ channel
TRAAK	TWIK Related Arachidonic Acid stimulated K^+ channel
TREK	TWIK Related K^+ channel
Tris	Tris-(hydroxymethyl)-aminomethan
TWIK	Tandem of P domains in a Weak Inward rectifying K^+ channel
TALK	TWIK related Alkaline pH activated K^+ channel
U	Units

Acknowledgements

First of all, I would like to present my gratitude to Prof. Jürgen Daut for giving me opportunity to work on tandem pore domain potassium channels and for his instruction and help.

I appreciate Dr. Regina Preisig-Müller for molecular biology works. I also acknowledge Bs. Marylou Zuzarte for her generous help and excellent work on immunohistochemistry.

I thank Vitaly Dyachenko and Gerrit Isenberg from Julius-Bernstein-institute for physiology of University Halle and Dr. Caroline Putzke from Klinikum of University Marburg for excellent whole cell recording in rat ventricular myocytes.

I also appreciate all my lab members-Susanne. Günter, Peter, Niels, Gao, Vijay, Frau Burk, Robert, Lothar……

Verzeichnis der akademischen Lehrer

Meine akademischen Lehrer waren die Damen/ Herren

in Marburg:

Daut

in Hubei:

Bao, Bai, Du, Fu, Fan, Feng, Gong, Han, Ji, Jin, Kong, Li, Liang, Mao, Nie, Qian, Qin, Rao, Sun, Tang, Wang, Wu, Yang, Ye, Yin, Zhao, Zhang, Zhou, Xiong.